IDENTIFICATION OF C17ORF45 PROTEIN AND THE EFFECTS OF ITS SNO-RNAS ON CELL CYCLE

by

Vahap Kapıkıran

B.S., Molecular Biology and Genetics, Boğaziçi University, 2010

Submitted to the Institute for Graduate Studies in
Science and Engineering in partial fulfillment of
the requirements for the degree of
Master of Science

Graduate Program in Molecular Biology and Genetics
Boğaziçi University

2013

IDENTIFICATION OF C17ORF45 PROTEIN AND THE EFFECTS OF ITS SNO-RNAS ON CELL CYCLE

APPROVED BY:

Assist. Prof. Necla Birgül İyison .....
(Thesis Supervisor)

Cemalettin Bekpen, Ph.D. .....

Prof. Arzu Karabay Korkmaz .....

DATE OF APPROVAL: 28.06.2013

To my wife and to my family...

ACKNOWLEDGEMENTS

I would like to thank my thesis supervisor, Assist. Prof. Necla Birgül İyison, for her guidance and support which made me highly motivated.

I would like to thank my thesis juries, Cemalettin Bekpen, Ph.D. and Prof. Arzu Karabay Korkmaz for spending their time to evaluate this thesis. I also would like to express my gratitude to Cemalettin Bekpen for his guidance and help in bioinformatics analyses.

Tuncay Şeker, who is my labmate and my advisor, deserves the greatest thanks for his great guidance and contributions to this thesis. He thought me not only lots of experimental techniques but also showed the way to think analytically.

My other labmates, İzzet Akiva, Burçin Duan Şahbaz, Esra Şekerci, Ruçhan Karaman, Emine Dindar and İpek Even, made the lab more enjoyable and I am also thankful to them for their valuable discussions.

I would like to thank Levent Baş to help me about writing this thesis in terms of guiding me about the writing format of the thesis.

I also would like to thank my closest friends Erdem Yılmaz and Mustafa Can Ayhan both for their perfect friendships and their helps in FACS analyses. I also would like to thank my other closest friends Uğur Kaplan, Güner Kaçmaz, Balkan Canher, Güneş Tunçgenç, Ekin Ece Erkan and Ayşegül Taşcı for their great supports and wonderful friendships.

I would like to thank my mother and my father for their unlimited supports and encouragements throughout my life.

The notable thanks and appreciations are for my wife, Pelin Aksoy Kapıkıran, who always supported and motivated me and who was with me during all my most difficult times.

Finally, I would like to thank TÜBİTAK-BİDEB (2210) to financially support me during my Master study.

This work was supported by The Scientific and Technological Research Council of Turkey (TÜBİTAK) Fund TBAG-211T182.

ABSTRACT

IDENTIFICATION OF C17ORF45 PROTEIN AND THE EFFECTS OF ITS SNORNAS ON CELL CYCLE

The Wnt / β-catenin signaling has many important roles in cellular responses and dysregulation of this pathway are linked to tumor formation. Priorly, SAGE and microarray analyses were performed in our laboratory in order to detect differentially expressed genes in Wnt / β-catenin pathway and *c17orf45* gene was found to be upregulated in the presence of constitutively active β-catenin. It was characterized as a novel Wnt / β-catenin target. A bioinformatics tool designed by our former lab member was used to detect differentially expressed genes in different tumor samples from online data. This indicated that the expression level of *c17orf45* gene was altered in distinct tumors. Besides, the upregulation of *c17orf45* was experimentally observed in meningioma samples. Moreover, *c17orf45* gene is accepted as the host gene for 3 snoRNAs in its introns. SnoRNAs are mainly involved in post-transcriptional modification of ribosomal RNAs; however the roles of snoRNAs in cancer are currently identified. In this study, the putative protein product of *c17orf45* gene and the effects of 2 snoRNAs residing in introns of *c17orf45* on different cancer cells were analyzed. Bioinformatics and PAML analyses for *c17orf45* ORF revealed that there might be a positive selection for putative protein of the gene. Western Blot analysis done to identify the putative protein resulted in that the antibody did not target the protein of *c17orf45*. Besides, to examine the possible effects of snoRNAs, snoRNAs were cloned into intronic region of *HBB* gene encompassed by exonic parts in order to splice intron out. This would lead to obtain functional, processed snoRNAs. Splicing were verified with RT-PCR, Real Time PCR and YFP fused HBB construct which depended on joining of exons and splicing out of intron. Then, snoRNA constructs were introduced to different cancer cell lines to determine the effects of snoRNAs on cell cycle. However, none of the cells with 2 different time points indicated an alteration on cell cycle.

ÖZET

C17ORF45 GENİNİN PROTEİNİNİ BELİRLEME VE SNORNA'LARININ HÜCRE DÖNGÜSÜ ÜZERİNDEKİ ETKİSİ

Wnt / beta-katenin sinyal yolağının hücre üzerinde önemli etkileri vardır ve bu yolak ve bileşenleri üzerindeki düzensizlikler kanser ile ilişkilendirilmiştir. Daha önce laboratuvarımızda yapılan SAGE ve mikroarray analizleri ile Wnt / beta-katenin yolağında anlatımı değişen genler bulunmuş ve hücreye aktif beta-katenin verildiğinde *c17orf45* geninin anlatımının arttığı gözlenmiştir. Ayrıca bu gen Wnt yolağı hedef geni olarak da belirlenmiştir. Bunun yanı sıra, farklı kanser türlerinde anlatımı değişen genleri belirlemek amacıyla geliştirilen bir biyoinformatik program vasıtasıyla *c17orf45* geninin anlatımının bir çok kanser türünde farklılık gösterdiği saptanmıştır. Laboratuvarımızda gerçekleştirişen başka bir çalışmada ise genin anlatımının menenjiyom örneklerinde arttığı gözlenmiştir. Bunula beraber, *c17orf45* geni intronik bölgelerinde 3 farklı snoRNA barındırdığı bilinmektedir. SnoRNA'ların asıl görevlerinin rRNA üzerindeki translasyon sonrası modifikasyonlarda görev almak olduğu kabul edilse de son zamanlarda snoRNA'ların kanser oluşumundaki rolü belirlenmiştir. Bu çalışmada, c17orf45 geninin olası proteini ve snoRNA'larının hücre döngüsü üzerindeki etkisi araştırılmıştır. PAML analizi bu genin işlevsel bir protein üretebileceğini işaret etmesine rağmen Western blot sonuçları kullanılan antikorun olası proteini tanımadığını göstermiştir. Ayrıca, snoRNA'ların kanser hücreleri üzerindeki etkisini görmek amacıyla genin snoRNA'ları *HBB* geninin intronik bölgesine klonlanmış ve eksonların uç uca eklenmesi sonrası introndan fonksiyonel snoRNA'ların çıkması hedeflenmiştir. Bu bağlamda yapılan deneyler pozitif sonuç vermiş olup bir sonraki aşamada snoRNA'ların hücre döngüsü üzerindeki olası etkileri farklı kanser hücre hatları üzerinde analiz edilmiş; ancak hiç bir hücre hattında belirgin bir fark gözlenememiştir.

TABLE OF CONTENTS

LIST OF FIGURES

LIST OF TABLES

LIST OF SYMBOLS

bp	Base Pairs
cm	Centimeter
g	Gravity
gr	Gram
kDa	Kilodalton
mg	Milligram
min	Minute
ml	Milliliter
mm	Millimeter
mM	Millimolar
ng	Nanogram
nm	Nanometer
u	Unit
V	Volt
°C	Centigrade degree
µg	Microgram
µl	Microliter
β	Beta

LIST OF ACRONYMS / ABBREVIATIONS

APC	Adenomatous polyposis coli
APS	Ammonium persulfate
BSA	Bovine Serum Albumin
$CaCl_2$	Calcium Chloride
cDNA	Complementary DNA
ChIP	Chromatin Immuoprecipitation
CK1	Casein kinase 1
CO_2	Carbon dioxide
DEPC	Diethylpyrocarbonate
DMEM	Dubecco's Modified Eagle Medium
DMSO	Dimethyl sulfoxide
DNA	Deoxyribonucleic Acid
dNTP	Deoxyribonucleosidetriphosphate
Dvl	Dishevelled
EDTA	Ethylenediaminetetraacetate
EtOH	Ethanol
FAP	Familial adenomatous polyposis
FBS	Fetal Bovine Serum
Fz	Frizzled
gDNA	Genomic DNA
GFP	Green Fluorescent Protein
GSK3β	Glycogen synthase kinase-3-beta
HBB	Beta Globin
HRP	Horseradish Peroxidase
LB	Luria-Bertani
LEF	Lymphoid enhancer factor
LRP	Low density lipoprotein receptor-related protein
MEGA	Molecular Evolutionary Genetics Analysis
MGC	Mammalian Gene Collection

$MgCl_2$	Magnesium chloride
miRNA	Micro RNA
NaOAc	Sodium Acetate
ORF	Open reading frame
PAGE	Polyacrylamide Gel Electrophoresis
PAML	Phylogenetic Analysis by Maximum Likelihood
PBS	Phosphate Buffered Saline
PCR	Polymerase Chain Reaction
PI	Propodium Iodide
PVDF	Polyvinylidene Fluoride
RISC	RNA Interference Silencing Complex
RNA	Ribonucleic Acid
rpm	Revolution per minute
RT	Room Temperature
RT-PCR	Reverse Transcriptase PCR
SAGE	Serial analysis of gene expression
SDS	Sodium dodecyl sulfate
snoRNA	Small nucleolar RNA
TCF	T-cell factor
TEMED	Tetramethylethylenediamine
YFP	Yellow Fluorescent Protein

1. INTRODUCTION

1.1. The Wnt Signaling Pathway

The Wnt signaling pathway has crucial roles in different mechanisms such as proliferation, differentiation, apoptosis, development and tissue homeostasis (Brocardo and Henderson, 2008, Clevers, 2006, Nusse, 2008, Valdivia *et al.,* 2011). The pathways can be classified according to their dependency on β-catenin. The canonical Wnt / β-catenin signaling pathway is the best characterized compared to non-canonical Wnt signaling pathways. The canonical Wnt / β-catenin pathway is stimulated by binding of a Wnt ligand to its coreceptors, Frizzled (Fz) and low-density lipoprotein receptor-related protein 5 or 6 (LRP5 or LRP6) (Clevers, 2006). Interaction between Wnt ligand and receptors triggers the interaction of Axin and LRP5 (Mao *et al.,* 2001) with the help of recruitment of Dishevelled (Dvl) (Chen *et al.,* 2003, Zeng *et al.,* 2008). The movement of Axin to the receptor complex leads not to constitute the degradation complex consisting of Adenomatous polyposis coli (APC), glycogen synthase kinase-3-beta (GSK3β) and casein kinase 1 (CK1). The deficiency of destruction complex causes β-catenin to translocate to the nucleus. In nucleus, β-catenin forms a transcription complex with T cell factor (TCF) and lymphoid enhancer factor (LEF). This complex provides the transcription of Wnt target genes (He *et al.,* 1998, Molenaar *et al.,* 1996).

However, when there is no Wnt ligand, destruction complex can form and this leads to phosphorylation of β-catenin. β-catenin is phosphorylated at different sites in its N-terminus (Sakanaka, 2002, Yost *et al.,* 1996). These phosphorylations mark β-catenin for ubiquitination and that results in proteosomal degradation (Aberle *et al.,*1997). The canonical Wnt signaling is illustrated in Figure 1.1.

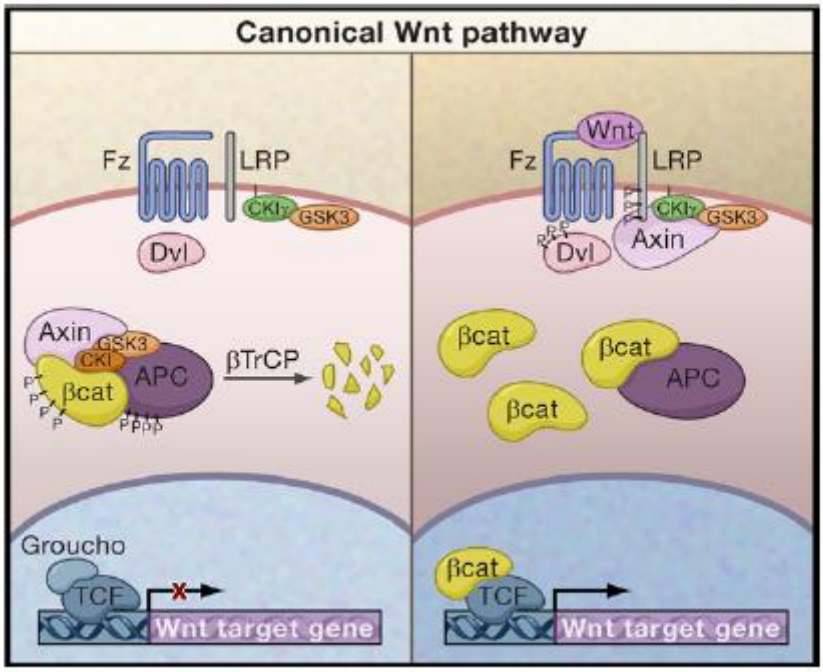

Figure 1.1. The canonical Wnt signaling with off (left) and on (right) states (Adapted from Clevers, 2006).

Dysregulation of the Wnt signaling and mutations in the components of the pathway are associated with many different cancer types (Klaus and Birchmeier, 2008). APC mutations are found in familial adenomatous polyposis (FAP) and colorectal cancer patients (Nishisho *et al.,* 1991). Axin mutations is also observed in colorectal cancer (Liu *et al.,* 2000) and hepatocellular carcinoma (Satoh *et al.,* 2000). The core component of Wnt signaling, which is β-catenin, has been showed to have a role in various cancer types due to its phosphorylation sites on its N-terminal residues (Polakis, 2000).

1.2. *C17Orf45* Gene

C17orf45 gene was initially defined in Mammalian Gene Collection (MGC) project of National Institute of Health (NIH). The main aim of this project was to constitute the clones of complete ORF of any human gene (Gerhard *et al.,* 2004). By MGC project, the hypothetical protein product of *c17orf45* gene was identified as 130 amino ac-

ids. Currently, the gene was annotated as *c17orf76-AS1* (Gene ID: uc002gqc.3, UCSC Genome Browser; Gene ID: 125144, GenBank).

Previously in our laboratory, SAGE and microarray analyses were performed to indicate differentially expressed genes in Wnt / β-catenin pathway. According to the results of SAGE and microarray, upregulation of *c17orf45* mRNA was observed in a hepatocellular carcinoma cell line, Huh7, which was transfected with mutant and constitutively active form of β-catenin (Kavak, 2009). In another study performed in our laboratory, *c17orf45* gene was identified and characterized as a novel Wnt / β-catenin target gene. In that study, lithium treatment assay which mimicked active Wnt signaling indicated an increase in mRNA level of *c17orf45* gene. The promoter analysis for *c17orf45* performed with luciferase assay showed a significant increment compared to control. Also, ChIP assay revealed that β-catenin interacts with the promoter region of *c17orf45* (Şeker, 2009). Besides, the possible relationship of this gene with tumorigenesis was also analyzed. A bioinformatics program called as oncoreveal, designed by Erşen Kavak (Kavak *et al.,* 2010), identified *C17orf45* gene as differentially expressed in different tumor samples (Kavak, 2009). Upregulation of the gene was observed mainly in brain tumor especially for meningioma samples (Şeker, 2009). In addition to this, novel oncogenic candidate genes in osteosarcoma located in 17p11.2-p12 chromosomal location where *c17orf45* gene resides were determined. *C17orf45* gene was identified with high copy number variation and high expression level that makes the gene a candidate for oncogene in osteosarcoma (Both *et al.,* 2012). Apart from these, *c17orf45* is the host gene for three small nucleolar RNAs locating in its introns and regulates their transcriptions.

1.3. Small Nucleolar RNA

1.3.1. General Features of SnoRNAs

Small nucleolar RNAs (snoRNAs) are non protein coding RNAs composed of 60-300 nucleotides. SnoRNAs mainly involve in the regulation of modifications of ri-

bosomal RNAs as post-transcriptionally (Bratkovic and Rogelj, 2011). These modifications include 2'-*O*-ribose methylation and pseudouridylation (Bachellerie *et al.,* 2002). Sno-RNAs responsible for these modifications can be defined according to their consensus motifs: C/D box and H/ACA box (Figure 1.2). C/D box snoRNAs have C box (RUGAUGA, R stands for A or G and D box (CUGA) close 5' and 3' terminus, respectively (Bratkovic and Rogelj, 2011). C and D box come close to each other with the help of 5' and 3' terminus having a complementary site to each other called as stem box structure and which all is crucial for biogenesis of snoRNA (Cavaille and Bachellerie, 1996, Huang *et al.,* 1992). In addition to C and D box, C' and D' boxes are also found in C/D box snoRNAs. Upstream of D and D' boxes, there are antisense elements which have complementary sequence to target RNA primarily for methylation. H/ACA box sno-RNAs, similar to C/D box snoRNAs, have consensus motifs called H box (ANANNA, N stands for any nucleotide) and ACA box (Bratkovic and Rogelj, 2011). H/ACA box snoRNAs consist of two hairpin domains and generally one of them contain the internal loop including the complementary bases to target RNA, required for pseudouridylation (Bortolin *et al.,* 1999, Ganot *et al.,* 1997).

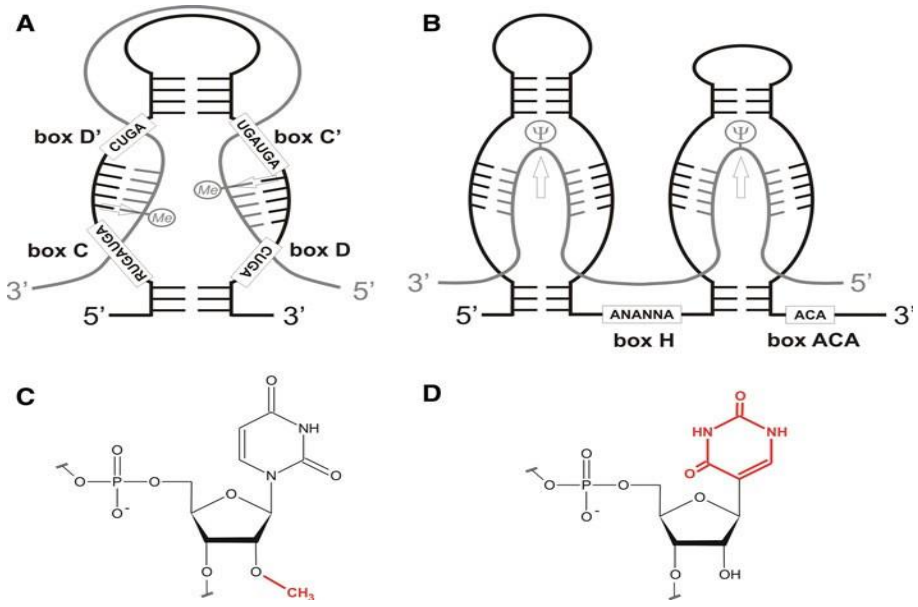

Figure 1.2. C/D box and H/ACA small nucleolar RNAs.Consensus sequences and target RNA modifications are indicated (Adapted from Bratkovic and Rogelj, 2011).

SnoRNA transcription can be regulated in two ways: snoRNAs can be transcribed either from independent promoters under the control of RNA polymerase II or they might be obtained from the introns of the protein coding or non-protein coding genes (Bratkovic and Rogelj, 2011). Most of human snoRNAs are intron encoded. The host genes of these snoRNAs mainly regard to 5' terminal oligopyrimidine gene family that have function related to ribosome or translation (Smith and Steitz, 1998, Yamashita *et al.,* 2008). Host genes of intronic snoRNAs having no protein coding potential was previously thought that their only function is the being host to snoRNAs; however non-protein coding host genes might have important function in cellular responses (Askarian-Amiri *et al.,* 2011, Kino *et al.,* 2010).

1.3.2. Cellular Functions of SnoRNAs

Main functions of snoRNAs are 2'-*O*-ribose methylation and pseudouridylation on target RNA. There are other snoRNAs, which have different functions e.g. HBII-52, a C/D box snoRNA located in deleted chromosomal region in Prader-Willi syndrome. It has an antisense strand with a perfect complementarity to human seratonin receptor, 5-HT_{2c}R. The main function of this snoRNA is to have a role in the alternative splicing regulation of seratonin receptor and HBII-52 is required to obtain functional seratonin receptor (Kishore and Stamm, 2006). Besides, the mouse homolog of HBII-52, MBII-52, was shown to have a function in RNA editing (Vitali *et al.,* 2005). Likewise, another C/D box snoRNA HBII-180C has a function to regulate the alternative splicing of FGFR3 (Scott *et al.,* 2012).

In addition to the role of snoRNAs in alternative splicing and RNA editing, it recently demonstrated that snoRNAs have significant affects in tumorigenesis and cancer development. A C/D box snoRNA called U50 is located in the genomic locus where it is deleted in many different cancer types, they might have a tumor suppressive role in prostate cancer. Mutation in snoRNA U50 was detected in multiple samples. It is downregulated in tumor samples and wild type form of U50 inhibits cellular proliferation and colony formation (Dong *et al.,* 2008). Similarly, U50 snoRNA was associated with breast cancer formation (Dong *et al.,* 2009) and B cell lymphoma because of its

location at chromosomal breakpoint (Tanaka *et al.,* 2000). Besides, snoRNA with potential oncogenic characteristic might have a participation in lung cancer was also specified. Overexpression of snord33, snord66, snord76 and snora42 were primarily determined in lung tumor samples (Li *et al.,* 2006). Among these, snora42 was shown to act as a oncogene. Downregulation of snora42 inhibit the proliferation and colony formation with *p53* dependent manner and its ectopic expression increases the proliferation and colony formation (Mei *et al.,* 2012).

Another snoRNA function distinct from its canonical roles is that smaller RNAs might be derived from snoRNA and these smaller RNAs can act as miRNAs to downregulate target mRNA expression. ACA45 snoRNA was shown to process into smaller RNA, associated with RNA Interference Silencing Complex (RISC) proteins and downregulate target mRNA expression (Ender *et al.,* 2008). Some other snoRNAs were also indicated as similar function (Brameier *et al.,* 2011). Moreover, many different miRNAs have been shown that they remind C/D or H/ACA box snoRNAs (Ono *et al.,* 2011, Scott *et al.,* 2009). It might possibly result from the evolutionary relationship between sno-RNAs and miRNAs (Scott and Ono, 2011).

1.3.3. Intron Encoded SnoRNAs of *C17Orf45* Gene

C17orf45 is a host gene for 3 different snoRNA residing in its introns. These snoRNAs are called as snord49a, snord49b and snord65 (HBII-135). Snord49a (GenBank Accession Number: X96649) was initially showed in a study that it was immunoprecipitated with fibrillarin, which was a protein associated with small nucleolar ribonucleoproteins (snoRNPs) and this snoRNA was predicted to have a role in 2'-*O*-ribose methylation of 28S rRNA at C4426 (Kiss-Laszlo *et al.,* 1996, Xie *et al.,* 2007). Snord49b is the truncated form of snord49a and have the exact function with full length forms (Kiss-Laszlo *et al.,* 1996, Lestrade and Weber, 2006). HBII-135 is the human ortholog of mouse MBII-135 and it might function in the methylation of 18S rRNA at U627 (Huttenhofer *et al.,* 2001, Xie *et al.,* 2007). Possible secondary structures of these snoRNAs were also determined and shown in Figure 1.3.

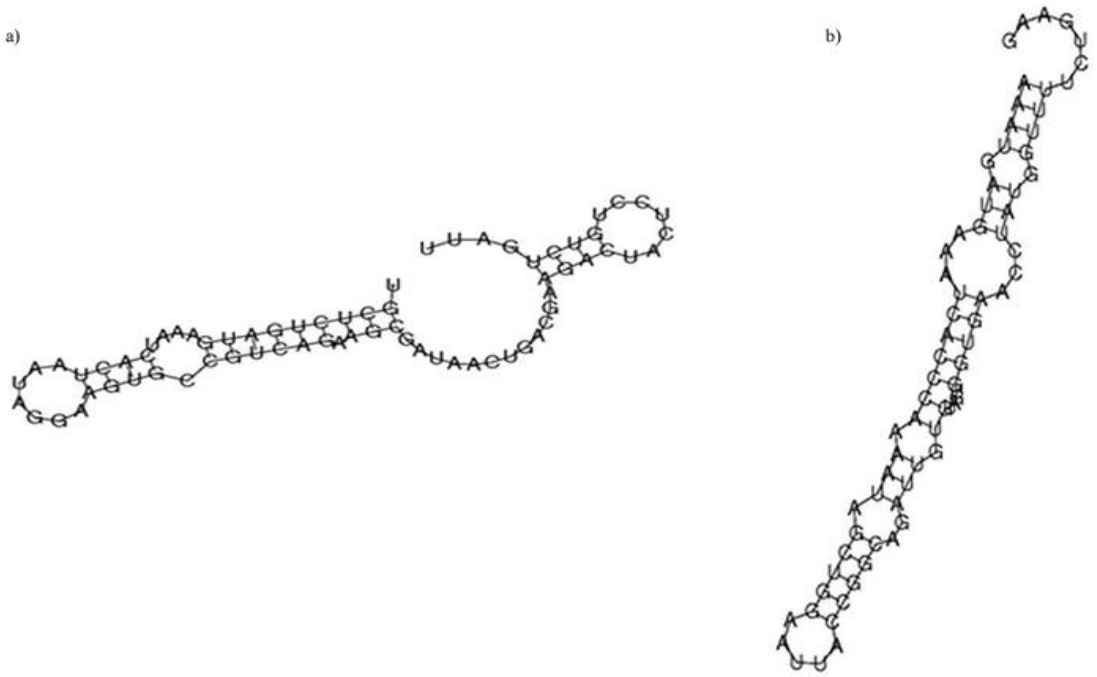

Figure 1.3. Predicted secondary structures of (a) snord49a and (b) snord65 (HBII-135) (Adapted from Xie *et al.*, 2007).

2. PURPOSE

The main aims of this study were to identify the putative protein of *c17orf45* gene and to analyze whether its snoRNAs within in intronic region had any impacts on cell cycle in different cancer cells.

Wnt / β-catenin signaling pathway is vital for many processes within the cell and the impairments in the pathway lead to cancer. Previous studies performed in our lab showed that c17orf45 gene was a novel transcriptional target of Wnt / β-catenin pathway. The relativity between the gene and tumorigenesis was observed. Besides, the constructs including ORF of the gene indicated phenotypic impacts on some cancer cell lines like inhibiting proliferation or colony formation when they introduced to the cells. Because previous studies on *c17orf45* gene suggested that it is able to encode a functional protein. In this regard, we performed bioinformatics analyses, Western Blot experiments and mass spectrometry analysis were performed in order to examine the putative product of the gene.

Furthermore, there are 3 snoRNAs in intronic region of *c17orf45* gene and snoRNA-cancer relationship was recently clarified. Hence, these snoRNAs residing in *c17orf45* gene were analyzed in terms of their possible effects on different cancer cells. In this context, 2 snoRNAs of the gene were cloned into second intron of *HBB* gene to characterize splicing the intron out which is required to obtain functional snoRNAs. Consequently, the effects of those snoRNAs on cell cycle were analyzed.

3. MATERIALS

3.1. General Kits, Enyzmes and Reagents

Table 3.1. List of kits, enzymes and reagents.

BCA Protein Assay Kit	Pierce, USA
DMEM	HyClone, USA
DNA Molecular Weight Marker	GeneRuler 1 kb DNA Ladder, Fermentas, USA ; 50 bp ladder, NEB, USA ; 100 bp ladder, NEB, USA
DNAse I (Recombinant)	Roche, Switzerland
FBS	HyClone, USA
GeneJET Plasmid Midiprep Kit	Thermo Scientific, USA
High Pure Plasmid Isolation Kit	Roche, Switzerland
ImProm-II Reverse Transcription System	Promega, USA
Light Cycler Fast Start DNA Master SYBR Green I kit	Roche, Switzerland
MinElute Gel Extraction Kit	QIAGEN, Germany
MinElute PCR Purification Kit	QIAGEN, Germany
Non Essential Amino Acid	HyClone, USA
Penicillin/Streptomycin	HyClone, USA
Phosphate Saline Buffer (PBS) - Cell Culture Grade	HyClone, USA
Protein A Agarose Beads	Pierce, USA
Protein Molecular Weight Marker	PageRuler Prestained Protein Ladder, Fermentas, USA
Restriction Eznymes	Fermentas, USA
T4 DNA Ligase	Roche, Switzerland
Taq DNA polymerase	Fermentas, USA
TriPure Isolation Reagent	Roche, Switzerland
Trypsin	HyClone, USA
Turbofect	Fermentas, USA
Western Blotting Luminol Reagent	Santa Cruz, USA

3.2. Biological Materials

3.2.1. Bacterial Strains

Escherichia coli TOP10 strain was used for the transformation experiments. The genotype of *Escherichia Coli* TOP10 strain is F-mcrA Δ(mrr-hsdRMS-mcrBC) Φ80lacZΔM15 ΔlacX74 recA1 araD139 Δ(araleu) 7697 galU galK rpsl (StrR) endA1 nupG.

3.2.2. Cell Lines

Huh7, Hep3B (human hepatocellular carcinoma; kindly provided by Dr. Mehmet Öztürk), U373-MG (human astrocytoma; kindly provided by Dr. P.O. Couraud), HeLa (human cervical cancer cell line; kindly provided by Dr. Cemalettin Bekpen), HEK293FT (human embryonic kidney cell line; kindly provided by Dr. Nesrin Özeren) and MCF-7 (human breast cancer cell line; kindly provided by Dr. N.C. Tolga Emre) cell lines were used.

3.2.3. Plasmids

pcDNA3 (Invitrogen, CA, USA), pEGFP-N2 (Clontech, CA, USA), pIRES2-EGFP (Clontech, CA, USA), pcDNA4-HisC (Invitrogen, CA, USA), pEYFP-N1 (Clontech, CA, USA) plasmids were used.

3.2.4. Primers

Table 3.2. Primers used in this study.

Primer ID	Sequence	Application
HBB_exon2_fwd_hind3	GGGAAGCTTTGAGAACTTCAGGGTG AGTCTA	Cloning
HBB_intron2_rev_newMCS	GGATCCTGGTACCTGAATTCACATTA CACTTTAACCC	Cloning
HBB_intron2_fwd_newMCS	AAAGAATTCAGGTACCAGGATCCGTG TACACATATTGACCAA	Cloning
HBB_exon3_rev_Xba1	TTTTCTAGATTTGCCAAAGTGATGGGC CAGCA	Cloning
SNORD49A_fwd_EcoR1	GGGGAATTCCTTGACTGCTCTGATGAA ATCACTAA	Cloning, RT&Q-RT-PCR
SNORD49A_rev_BamH1	TTTGGATCCCTTGACTGCAATCAGACA GGAGTAG	Cloning, RT&Q-RT-PCR
SNORD65_fwd_EcoR1	GGGGAATTCAGATATCAAATGATGAA ATCACCCAAAAT	Cloning, RT&Q-RT-PCR
SNORD65_rev_BamH1	TTTGGATCCAGATATCTTCAGAAAACC ATAGGTTCACC	Cloning, RT&Q-RT-PCR
HBB_e2fwd_GFP_Bgl2	AAAAGATCTATGCCTGAGAACTTCAGG GTGAGTCTATGG	Cloning
HBB_e3rev_GFP_Hind3	TTTAAGCTTTTTGCCAAAGTGATGGGCC AGCA	Cloning
HBB_spliced_RT_Fwd	GGATCCTGAGAACTTCAGG	RT& Q-RT-PCR
HBB_spliced_RT_Rev	TTTGCCAAAGTGATGGGCC	RT& Q-RT-PCR

3.3. Chemicals

Table 3.3. Chemicals used in this study.

Acetic Acid	Riedel de Haen, Germany
Acrylamide	AppliChem, Germany
Agar	Conda, Spain
Agarose E	Conda, Spain
Ammonium Persulfate (APS)	Sigma-Aldrich, USA
Ampicillin	AppliChem, Germany
Bovine Serum Albumin (BSA)	AppliChem, Germany
Bromophenol Blue	Fluka, USA
Calcium chloride dihydrate	AppliChem, Germany
Chloroform	Sigma-Aldrich, USA
Coomassie Brilliant Blue (R-250)	Sigma-Aldrich, USA
DMSO	Sigma-Aldrich, USA
EDTA	AppliChem, Germany
Ethanol	Emsure, Germany
EZMix Tryptone	Sigma-Aldrich, USA
Glycerol	Sigma-Aldrich, USA
Glycine	Fisher Scientific, USA
Isopropanol	Emsure, Germany
Kanamycin	Fluka, USA
Methanol	Emsure, Germany
N, N, N', N'-tetramethylethylenediamine (TEMED)	AppliChem, Germany
N,N'-Methylenebisacrylamide	Sigma-Aldrich, USA
NP-40	Roche, Switzerland
Phenol:chloroform:isoamyl alcohol (125:24:1)	Fluka, USA
Phosphate Saline Buffer (PBS) - Mol. Biology Grade	Gibco, UK
Sodium Chloride (NaCl)	Fisher Scientific, USA
Sodium Dodecyl Sulfate (SDS)	AppliChem, Germany
Tris-Base	AppliChem, Germany
Tris-Cl	AppliChem, Germany
Tween 20	Sigma-Aldrich, USA
Yeast Extract	Conda, Spain

3.4. Buffers and Solutions

Table 3.4. Buffers and solutions used in this study.

10X SDS Running Buffer	1% SDS 1.92M Glycine 250 mM Tris-Base
10X Transfer Buffer	1.92M Glycine 250 mM Tris-Base
1X Transfer Buffer	10% 10X Transfer Buffer 20% Methanol
20X SB Buffer	730 mM Boric Acid 200 mM NaOH
4X Protein Loading Dye	200 mM Tris-Cl (pH: 6.8) 8% SDS 40% Glycerol 4% β-mercaptoethanol 50 mM EDTA 0.8% Bromophenol Blue
Cell Lysis Buffer	137 mM NaCl 20 mM Tris-Cl (pH: 7.4) 2 mM EDTA 0.2 % NP-40 5 mM NaF
Coomassie Blue Destaining Solution	30% Isopropanol 10% Acetic Acid
Coomassie Blue Fixation Solution	50% Methanol 10% Acetic Acid
Coomassie Blue Staining Solution	50% Methanol 10% Acetic Acid 0.05% Coomassie Blue R-250
DNA Loading Buffer	10 mM Tris-Base (pH: 7.4) 0.03% Bromophenol Blue 0.03% Xylene Cyanol 60% Glycerol 60 mM EDTA
LB	5 g/l NaCl 10 g/l Tryptone 5 g/l Yeast Extract

Table 3.4. Buffers and solutions used in this study (cont.).

LB Agar	5 g/l NaCl 10 g/l Tryptone 5 g/l Yeast Extract 15 g/l Agar
Propodium Iodide Staining Solution	20 µg/ml Propodium Iodide 0.1% Triton X-100 dissolved in 1X PBS
TBS-T	50 mM Tris-Base (pH: 7.4) 150 mM NaCl 0.1% Tween 20

3.5. Antibodies

Table 3.5. Antibodies used in this study.

Name	**Species**	**Dilution**	**Source**
Anti-c17orf45 (sc-136581)	Rabbit	1/500	Santa Cruz
Anti-GFP HRP linked (sc-8334)	Rabbit	1/500	Santa Cruz
Anti-myc (#2272)	Rabbit	1/1000	Cell Signaling
Anti-beta actin (#4970)	Rabbit	1/1000	Cell Signaling

3.6. Disposable Labware

Table 3.6. List of disposable labwares used in this study.

Cell culture plates, 10 cm	Thermo, USA
Cell culture plates, 145 mm	Thermo, USA
Cell culture plates, 6 well	Thermo, USA
Cell culture plates, 96 well	Thermo, USA
Cell scraper	TPP, Switzerland

Table 3.6. List of disposable labwares used in this study (cont.).

Cryo tubes	Greiner Bio One, UK
Filtered tips	Axygen ,USA
Insulin syringes	Set Medikal, Turkey
PCR tubes, 0.2 ml	Axygen ,USA
Pipette tips	Axygen ,USA
Test tubes, 1.5 ml	Axygen ,USA
Test tubes, 2 ml	Axygen ,USA
Test tubes, 15 ml	TPP, Switzerland
Test tubes, 50 ml	TPP, Switzerland

3.7. Equipment

Table 3.7. List of equipment used in this study.

Autoclave	Midas 55,Prior Clave, UK
Carbon dioxide Tank	2091, Habaş, Turkey
Cell Culture Incubator	Hepa Class 100, Thermo, USA
Centrifuges	J2-21, Beckman Coulter, USA Allegra X-22, Beckman Coulter, USA 5415R, Eppendorf, USA
Documentation System	GelDoc XR System, Bio-Doc, Italy
Flow Cytometer	FACSCalibur , Becton Dickinson, USA
Freezers	−20°C, Arçelik, Turkey −80°C ULT Freezer, ThermoForma, USA
Heat Block	DRI-Block DB-2A, Techne, UK
Micropipettes	Finnpipette, Thermo, USA
Microplate Reader	680, Biorad, USA
Microscopes	Inverted Microscope, CKX41, Olympus, JAPAN Fluoroscence Microscope, Observer.Z1, Zeiss, Germany
Microwave	MD554, Arçelik, Turkey
PCR Machine	Gene Amp. PCR System 2700, Applied Biosystems, USA
Power Supply	Biorad, USA
Real Time PCR	LightCycler 1.5, Roche, SWITZERLAND
SDS Gel Electrophore-sis	Biorad, USA
Shaker	VIB Orbital Shaker, InterMed, DENMARK
Spectrophotometer	NanoDrop 1000, USA

Table 3.7. List of equipments used in this study (cont.).

Stella	Raytest, Germany
Vortex	Vortexmixer VM20, Chiltern Scientific, UK

4. METHODS

4.1. Bioinformatics Methods

4.1.1. Extracting the Sequences of ORF of *C17Orf45* Gene and Its snoRNAs from Genome Browser Database

Open reading frame (ORF) of *c17orf45* gene (uc002gqc.3) was taken from UCSC Genome Browser Database (Meyer *et al.,* 2013) and Blat Search was performed for different species (Kent, 2002). According to Blat Search results, putative ORFs of the gene for each species were taken. Besides, coding regions for snord49a and snord65 for distinct species was taken from database (Vertebrate Multiz Alignment) by utilizing human snord49a and snord65.

4.1.2. Construction of Phylogenetic Tree for ORF of *C17Orf45* Gene and Its snoRNAs

Putative ORF of *c17orf45* gene extracted from the genome of accessible species were aligned by using ClustalW server of EBI (Larkin *et al.,* 2007) without considering stop codon presence. Alignment file was utilized in MEGA5 software (Tamura *et al.,* 2007). File was used to a construct a phylogenetic tree with Neighbor-Joining method (Saitou and Nei, 1987) with Kimura-2 parameter (Kimura, 1980). The bootstrap test with 1000 replications was also applied (Felsenstein, 1985). Second phylogenetic tree was also constructed. Putative ORF of *c17orf45* gene for distinct species were taken and ORFs of the species were chosen till stop codon by translating sequences with ExPASy server of SIB (Artimo *et al.,* 2012). Nucleotide sequences of translated ORF were aligned and another phylogenetic tree was constructed with the same parameters above. Similarly, coding regions of snord49a and snord65 were taken and alignment was performed. Neighbor-Joining method with Kimura-2 parameter and 1000 replications for bootstrap were applied.

4.1.3. PAML Analysis

PAML analysis was performed to test evolutionary rates of the putative coding sequences of *c17orf45* gene extracted from the accessible genome databases for different species (Yang, 2007). To apply PAML analysis, three files were obligatory: a sequence file containing organized nucleotide sequences; a tree file containing phylogenetic tree of including species and a control file containing model and other parameters of the analysis. Sequence file was prepared after obtaining alignment file. Deleted bases even in a single species and stop codons within the frame were removed from all species. Tree file was prepared after obtaining from MEGA analysis. Acquired tree was corrected in TreeView software manually (Page, 1996). The ultimate tree file was used in PAML analysis. In test file, mainly the model of the test was chosen. Two different models were applied; one-ratio (one dN/dS ratio for whole tree) and free-ratio model (dN/dS ratio for each branch in the tree). The program was run in Windows/Dos.

4.2. Biochemical Methods

4.2.1. Cell Lysis and Protein Extraction from Different Cell Lines

To obtain basal level of protein or overexpressed proteins, cells in 6-well plate, 10 cm plate or 145 mm plate are washed once with 1X PBS. Lysis Buffer was added onto plates as 150 µl, 400 µl and 1000 µl for 6-well plate, 10 cm plate and 145 mm plate respectively. Plates were placed onto ice for 10 minutes. Cell scrapers were used to scrape cells and they were collected into 1.5 ml micro centrifuge tubes. They were incubated on ice for 1 hour. Insulin syringes were used to homogenize and get rid of genomic DNA. Cell lysates were centrifuged at 14000g for 20 minutes at 4°C. Supernatants obtained after centrifuged were transferred into fresh 1.5 ml micro centrifuge tubes. Protein lysates were stored at -20°C for short term storage or directly used.

4.2.2. Quantification of Protein Lysates

Protein quantification was performed by BCA Protein Assay Kit (Pierce). BSA standards was prepared via serial dilution to obtain different concentrations (125, 250, 500, 750, 1000, 1500 and 2000 µg/ml). Protein samples were prepared as 1/5 dilution in cell lysis buffer. All samples were prepared as duplicate. To prepare BCA Working Reagent, 50 parts Reagent A was mixed 1 parts Reagent B. For each sample, 150 µl of prepare BCA Working Reagent was prepared. They were added onto 96 well plate. Plate was placed onto ice. BSA standards and protein samples were added onto each well as 5 µl. Plate was incubated at 37°C for 30 minutes. Plate was cooled at RT for 5 minutes. The absorbance of samples was measured at 562 nm on the plate reader. Blank measurements were subtracted from the average 562 nm absorbance measurement. To calculate the concentration of samples, a standard curve was prepared by plotting blank corrected BSA measurements at 562 nm vs their corresponding concentrations in µg/ml. By using standard curve, concentration of each sample was calculated.

4.2.3. Preparation of Protein Lysates

Concentrations of each protein were adjusted according to the lowest amount of protein sample by means of addition of cell lysis buffer. 4X Protein Loading Dye was added into each sample and boiled at 95°C for 5 minutes.

4.2.4. Immunoprecipitation (IP)

For immunoprecipitation experiment, Huh7 cell line was used. Basal protein lysate was obtained as indicated in Section 4.2.1. Quantification of protein was determined as indicated in Section 4.2.2. 500 µg of protein lysate is mixed with 5 µl of anti-c17orf45 antibody in the total volume of 500 µl of lysis buffer. The protein-antibody mixture was incubated at 4°C for overnight by rocking. Next day, 40 µl of Protein A Agarose beads (Pierce) were washed twice with 300 µl of cell lysis buffer. Protein-antibody mixture was added onto agarose beads. This mixture was incubated at 4°C for

7 hours by rocking. The sample was centrifuged at 14000g for 10 minutes at 4°C. Supernatant was stored as control for Western Blot analysis. The beads were washed 4 times with 300 µl of 1X PBS. 1st wash supernatant was also kept as control. 4X Protein Loading Dye was added to beads and boiled at 95°C for 5 minutes.

4.2.5. SDS-PAGE

SDS-PAGE gel system was prepared with resolving gel polymerized at the bottom and stacking gel polymerized on the top of resolving gel. Bio-Rad gel electrophoresis system was used.

Table 4.1. Preparation of SDS-PAGE gels.

	Resolving Gel	**Stacking Gel**
ddH_2O	3.65 ml	1.825 ml
1M Tris-Cl (pH:6.8)	-	313 µl
1.5M Tris-Cl (pH:8.8)	2.25 ml	-
Acrylamide:Bisacrylamide (30% / 0.8% w/v)	3 ml	335 µl
SDS (20% w/v)	45 µl	13 µl
APS (10% w/v)	56.5 µl	21 µl
TEMED	13.5µl	6 µl

4.2.6. Western Blot

Protein samples were loaded into the wells and running was performed at 100 V for around 75 minutes. When run is complete, PVDF membrane was activated in methanol for 30 sec and was transferred into ddH_2O. SDS-PAGE was placed into transfer cassettes to obtain proteins on the membrane. Transfer was done at 100 V for 75 minutes at 4°C. When transfer was complete, membrane was blocked with 5% nonfat

dry milk in TBS-T for 1 hour at RT. The membrane was washed 3 times with TBS-T for 5 minutes. each. Primary antibodies were applied according to the manufacturer's protocol and prepared either in 5% non-fat dry milk or 5% BSA in TBS-T. Primary antibodies were incubated overnight at 4°C. Next day, membrane was washed 3 times with TBS-T for 5 minutes each. Secondary antibody, HRP-conjugated anti-rabbit IgG was prepared in 5% non-fat dry milk as 1:2000 diluted. Secondary antibody was applied at RT for 1 hour. Membrane was washed 3 times with TBS-T for 5 minutes each. To visualize the proteins, Western Blotting Luminol Reagent (Santa Cruz) was used as mixing Solution A and Solution B (1:1 ratio). The protein bands were visualized in bio/chemi-luminescence system (Raytest - Stella).

4.2.7. Coomassie Blue Staining

Protein samples were loaded into the wells and running was performed at 100 V for around 75 minutes. SDS gel was fixed with fixation solution at RT for 1 hour by shaking. Fixation solution was replaced with staining solution and incubated at RT for 20-30 minutes. When gel was stained totally, destaining solution was added and incubated until background color removed.

4.2.8. Preparation of Protein Sample for Mass Spectrometry

Protein bands obtained from Coomassie Blue Staining was cut via sterile razor blade and placed into 1.5 ml micro centrifuge tubes. Samples were stored at -80°C freezer until it was sent for analysis. Mass Spectrometry analysis was performed in "Institut für Klinische Chemie" in Hamburg.

4.3. Molecular Biological Techniques

4.3.1. Preparation of Chemically Competent Cells

5 ml of LB supplemented with 25 µg/ml of streptomycin was inoculated with *E.coli* TOP10 strain glycerol stock and grown at 37°C for overnight by shaking at 200 rpm. Next day, 50 ml of LB was inoculated with 500 µl of overnight culture (1:100). Cells were grown until OD at 600 nm reached to 0.4-0.6. Cells were centrifuged at 4000 rpm for 10 minutes at 4°C. The pellet was resuspended with 25 ml of autoclaved and ice-cold 50 mM $CaCl_2$ and incubated on ice for 30 minutes. Cells were centrifuged at 4000 rpm for 10 minutes at 4°C. The pellet was resuspended with 5 ml of the mixture of autoclaved, ice-cold 50 mM $CaCl_2$ and 10% glycerol (v/v). Aliquots were prepared as 100 µl for each and stored at -80°C freezer for longer use.

4.3.2. Transformation of Chemically Competent TOP10 Cells

A vial of competent cells was thawed on ice for 10 minutes and either 50 ng of plasmid or 1/5 amount of ligation mix was added onto cells. Cells were incubated on ice for 30 minutes. The vial was placed onto 42°C heat-block for 1 minute and then back onto ice for 2 minutes. 500 µl of LB was added onto cells and was grown at 37°C for 1 hours by shaking. 150 µl of cell suspension was spread out onto antibiotic containing agar plate and incubated at 37°C for overnight as in inverted position.

4.3.3. PCR Purification of DNA Samples

PCR products were purified with QIAGEN PCR Purification Kit. 5 volumes of Buffer PB was added onto 1 volumes of PCR product and mixed. The mixture was applied to the spin column and centrifuged for 1 minute. Supernatant was discarded and

the column was washed with 750 µl of Buffer PE. The samples were centrifuged for 1 minute. Supernatant was discarded and the column was centrifuged for an additional 1 minute. Column was placed into a sterile 1.5 ml micro centrifuge tube and 30 µl of pre-warmed elution buffer was added. It was centrifuged for 1 minute. The concentration and purity of DNA was determined via nanodrop.

4.3.4. Agarose Gel Extraction of DNA Samples

Agarose Gel Extraction was performed with QIAGEN Gel Extraction Kit. DNA sample was run in agarose gel and cut with a sterile razor blade and placed within a 1.5 ml micro centrifuge tube. DNA sample was weighted and 3 volumes of QG Buffer was added. The sample was placed into heat block at 50°C. It was incubated for approximately 10 minutes until all agarose dissolved. 1 volume of isopropanol was added and mixed well. The mixture was transferred into the spin column and centrifuged for 1 minute. The flow-through was discarded and the sample was washed with 750 µl of Buffer PE. It was centrifuged for 1 minute. Supernatant was discarded and the column was centrifuged for an additional 1 minute. Column was placed into a sterile 1.5 ml micro centrifuge tube 25 µl of pre-warmed elution buffer was added. It was centrifuged for 1 minute. The concentration and purity of DNA was determined via nanodrop.

4.3.5. Restriction Digestion of DNA

Digestion of DNA was performed by means of restriction enzymes (Fermentas) according to manufacturer's protocol. Restriction was usually done for 3 µg of plasmids with 3 unit of enzymes in 20 µl solution. Restricted DNA was purified either PCR purification or agarose gel extraction protocols.

4.3.6. Ligation

Ligations of plasmids and inserts were performed by means of T4 DNA Ligase (Roche) according to manufacturer's protocol. Ligations were usually done with 1 unit

of enzymes in 30 µl solution. Ligated products were purified with PCR purification protocols.

4.3.7. Colony PCR

To test the positive colonies after ligation, colony PCR was performed. The colonies chosen from agar plate were picked with a pipette tip and placed into PCR solution. After mixing within PCR solution, 1 µl of solution mix was dropped onto antibiotic resistant plate to create a backup plate. PCR was performed with 1X Taq Buffer, 2 mM $MgCl_2$, 0.5 mM dNTP mix, 0.4 µM of each primer, 8% DMSO, 1 u of home-made Taq polymerase. PCR products were run in 1% agarose gel.

4.3.8. Plasmid Isolation

To isolate plasmids, either miniprep or midiprep was applied. Miniprep was performed with High Pure Plasmid Isolation Kit (Roche). 5 ml of LB supplemented with the determined amount of antibiotic was inoculated with either the positive colony or glycerol stock for a sample. Sample was incubated at 37°C for overnight by shaking. Next day, cells were centrifuged at 4000 rpm for 15 minutes. The pellet was resuspended with 250 µl of Resuspension Buffer containing RNAse A and mixed. 250 µl of Lysis Buffer was added and mixed by inverting the tube 3-6 times. It was incubated at RT not more than 5 minutes. 350 µl of ice-cold Binding Buffer was added and mixed by inverting the tube 3-6 times. It was incubated on ice for 5 minutes and centrifuged at 13000g for 10 minutes. The supernatant was transferred into filter tube and centrifuged for 1 minute. Flow-through was discarded and 700 µl of Wash Buffer II was added. It was centrifuged for 1 minute. Flow-through was discarded and the filter tube was centrifuged for an additional 1 minute. Filter tube was placed into a sterile 1.5 ml micro centrifuge tube and 75 µl of pre-warmed Elution Buffer was added. It was centrifuged for 1 minute. The concentration and purity of DNA was determined via nanodrop.

Midiprep was performed with GeneJET Plasmid Midiperp Kit (Thermo). 50 ml of LB supplemented with the determined amount of antibiotic was inoculated with the interested bacterial glycerol stock for a sample. Sample was incubated at 37°C for overnight by shaking. Next day, cells were centrifuged at 4000 rpm for 30 minutes. The pellet was resuspended with 2 ml of Resuspension Buffer containing RNAse A and mixed. 2 ml of Lysis Buffer was added and mixed by inverting the tube 3-6 times. It was incubated at RT for 3 minutes. 2 ml of Neutralization Buffer was added and mixed immediately by inverting tube 5-8 times. 500 µl of Endotoxin Binding Reagent was added and mixed immediately by inverting tube 5-8 times. It was incubated at RT for 5 minutes. The sample was centrifuged at 15000 rpm for 30 minutes. Supernatant was transferred into a 15 ml tube and 1 volume of absolute ethanol was added. Sample was mixed and transferred into column containing collection tube. It was centrifuged at 2000g for 3 minutes. 4 ml of Wash Buffer I was added and centrifuged at 3000g for 2 minutes. Flow-through was discarded and 4 ml of Wash Buffer II was added. It was centrifuged at 3000g for 2 minutes. Washing step with Wash Buffer II was repeated once more. Flow-through was discarded and centrifuged at 3000g for additional 5 minutes. Column was transferred into new 15 ml tube and 350 µl of Elution Buffer was added. It was centrifuged at 3000g for 5 minutes. The concentration and purity of DNA was determined via nanodrop.

4.3.9. Total RNA Isolation

To obtain smaller size of RNA, TriPure Isolation Reagent (Roche) was used. Cells from 10 cm plate were washed with PBS and 500 µl of TriPure (Roche) reagent was added. Cell scraper was used to scrape cells. Cell lysate was mixed via pipetting several times and transferred into a 1.5 ml micro centrifuge tube. Sample was incubated at RT for 5 minutes. 200 µl of chloroform was added and shaked vigorously for 15 sec. It was incubated at RT for 5 minutes and centrifuged at 12000g at 4°C for 15 minutes. Upper, colorless aqueous phase was transferred into a fresh 1.5 ml micro centrifuge tube. 500 µl of isopropanol was added and mixed by inverting the tube several times. It was incubated at RT for 5-10 minutes to obtain precipitation. It was centrifuged at 12000g at 4°C for 10 minutes and supernatant was discarded. 500 µl of ice cold 75%

EtOH was added and vortexed. It was centrifuged at 7500g at 4°C for 5 minutes. Supernatant was discarded and excess ethanol was removed by air-drying. The pellet was resuspended with 85 µl of DEPC-treated RNAse free water. Sample was incubated with DNAse I and DNAse incubation buffer (Roche) in order to get rid of DNA within sample. It was incubated at 37°C for 30 minutes. When DNAse incubation finished, 260 µl of nuclease free water and 40 µl of 3M NaOAc (pH: 5.2) was added. 400 µl of acidic phenol:chloroform:isoamyl alcohol (125:24:1) was added and mixed quickly by inverting the tube several times. It was centrifuged at 12000g at 4°C for 12 minutes. Upper aqueous phase was transferred into a fresh 1.5 ml micro centrifuge tube. In order to minimize RNA loss, 100 µl of DEPC-treated water was added into mixture containing acidic phenol:chloroform:isoamyl alcohol and RNA and mixed. It was centrifuged at 12000g at 4°C for 12 minutes. Upper aqueous phase was also added into previous one. 500 µl of isopropanol was added and mixed. It was centrifuged at 12000g at 4°C for 12 minutes. Supernatant was discarded and pellet was dried. Pellet was washed with 1 ml of ice cold 75% EtOH and vortexed. It was centrifuged at 12000g at 4°C for 12 minutes. Pellet was dried and 50 µl of nuclease free water was added to resuspend the pellet. RNA sample was kept at -80°C freezer for later use.

4.3.10. Reverse Transcription and cDNA Synthesis

Reverse Transcription and cDNA synthesis were performed with Promega, ImProm-II Reverse Transcription System according to manufacturer's protocol. 1 µg of RNA was incubated at 70°C with 0.75 µl of oligo-dT primers and 0.75 µl of random primers with the addition of 2.5 µl of nuclease free water. Then, sample was incubated on ice for 5 minutes. Reverse transcription mix was prepared with 4 µl of reaction buffer, 5 µl of $MgCl_2$, 1 µl of dNTP mix, 0.5 µl of RNAse inhibitor, 1 µl of Reverse Transcriptase and 3.5 µl of nuclease free water. Reverse transcription mix was added onto RNA sample mix on ice and incubated at 25°C for 5 minutes. Then, sample mix was as incubated at 42°C for 1 hour. Enzyme inactivation was done at 70°C for 5 minutes. 80 µl of sterile nuclease free water was added to obtain 100 µl of reaction volume. Samples were stored at -20°C for later use.

4.3.11. RT-PCR

RT-PCR was performed with Taq DNA polymerase (Fermentas). Briefly, 1X Taq buffer, 8% DMSO, 2 mM of $MgCl_2$, 0.4 µM of each primers, 0.5 mM of dNTP mix, 1 u of Taq DNA polymerase, 40 ng of cDNA was prepared and PCR was performed.

4.3.12. Real Time PCR

Real Time PCR was performed with Roche, LightCycler Fast Start DNA Master SYBR Green I kit according to manufacturer's protocol. 2 µl of SYBR Green mix, 1 µl of primer mix, 1.5 µl of $MgCl_2$, 5 µl of cDNA and 10.5 µl of dH_2O was mixed and added into capillary. Standard curve was constructed for primers and cDNAs to calculate the efficiency. Results were analyzed with Light Cycler 4.0 Analysis Software (Roche) and Microsoft Excel (USA). Reaction started with initial denaturation at 95°C for 10 minutes. For elongation, there were 3 steps: denaturation at 95°C for 10 minutes, annealing at 57°C for 5 sec and elongation at 72°C for 5 sec. It was run for 45 cycles followed by a melting curve.

4.3.13. Cell Cycle Analysis

Cell cycle analysis was performed with different cell lines. Growth medium covering cells from 6 well plates were collected into 15 ml tubes. Cells are washed with 1X PBS and cells covered with PBS were also collected into same 15 ml tube. Trypsin was used to detach cells from plate. Growth medium was used to inactivate trypsin and detached cells were collected into same 15 ml tube. Cells were centrifuged at 1000g for 5 minutes. Supernatant was discarded and cells were washed with 1X PBS. To fix the cells, 5 ml of 70% EtOH was added onto cells with vortex. Cells were incubated on ice at least for 2 hours. Cells were centrifuged at 1000g for 5 minutes. 1 ml of PI stain containing 200 µg/ml of RNAse A was added onto cells. Cells within tube covered with aluminum foil in order to prevent direct light exposure were incubated at 37°C for 45

minutes. Cells were washed with 1X PBS and centrifuged at 1000g for 5 minutes. Cells were transferred into flow cytometer tubes and FACS analysis was performed.

4.4. Cell Culture Techniques

4.4.1. Growth Conditions of Cells

Cells used in cell culture were grown in DMEM – High Glucose containing 10% FBS, 1% of penicillin/streptomycin and 1% Non-essential amino acid. Cells were incubated in 5% CO_2 incubator at 37°C. Growth medium was kept at 4°C and warmed at 37°C before use.

4.4.2. Passaging

The cells were passaged either before experiments or before reaching to confluency. The growth medium was aspirated and cells were washed with 1X PBS. Trypsin (0.025%) was added onto the cells to remove cells from surface and incubated at 37°C for 3-5 minutes. 5 ml of growth medium was added to inactivate trypsin. Cells were centrifuged at 1500 rpm for 5 minutes. Cells were resuspended via pipetting. Determined amount of cells (generally as 1:5) were transferred into new Petri dishes.

4.4.3. Cryopreservation

Cells were removed from the surface with trypsin and inactivated with growth medium. Cells were centrifuged at 1500 rpm for 5 minutes. Cells were resuspended with 80% DMEM, 10% FBS and 10% DMSO mix. Fully confluent 10 cm plates were divided into four and 1 ml of solution containing cells were transferred into 2 ml screw capped-cyrotubes. Tubes were placed into NALGENE Cyro 1°C Freezing Container filled with isopropanol. Container provided cells to freeze -1°C/min. The container was placed into -80°C freezer.

4.4.4. Thawing

One vial of frozen cell were taken from -80°C freezer and placed into incubator at 37°C. Immediately after cells were thawed, cells were transferred into a 15 ml tube and 5 ml of growth medium was added. Cells were centrifuged at 1500 rpm for 5 minutes. Pellet was resuspended with sufficient amount of growth medium and transferred into a Petri dish.

4.4.5. Transient Transfection of Cells

Transfections were performed either in 6 well plates or 10 cm plates with *in vitro* Turbofect (Fermentas) reagent. Cells were seeded the day before transfection to get 50-60 per cent confluency at the day of transfection. For 6 well plate, 3 µg of plasmid DNAs and 300 µl of serum free medium was mixed in a sterile tube. 5 µl of transfection reagent was added onto plasmid-medium mixture. For 10 cm plate, 12 µg of plasmid DNAs and 1200 µl of serum free medium were mixed in a sterile tube. 18 µl of transfection reagent was added onto plasmid-medium mixture. Final mixture was vortexed, spinned down and incubated at RT for 20 minutes. The mixture was added onto the cells and the plate was swirled. The cells were incubated at 37°C either for 24 or 48 hours. The transfection media was replaced with fresh medium after 4 hours.

4.5. Construct Design for HBB Exon-Intron-SnoRNA

The construct for HBB exon-intron-exon was mentioned earlier (Kiss and Filipowicz, 1995) and slightly different strategy was applied. To do this, PCR amplification was performed for the part of exon 2 and the part of intron 2 of *HBB* gene for the first part of the construct. HindIII restriction site was added into 5’ of the forward primer (HBB_exon2_fwd_hind3) and EcoRI-KpnI-BamHI restriction sites were added into 5’ of the reverse primer (HBB_intron2_rev_newMCS). For the second part of the construct having the part of intron 2 and the part of exon 3, EcoRI-KpnI-BamHI restriction sites were added into 5’ of forward primer (HBB_intron2_fwd_newMCS) and XbaI re-

striction site was added into 5' of reverse primer (HBB_exon3_rev_Xba1). These two constructs were amplified from genomic DNA with Phusion High Fidelity DNA Polymerase (Thermo). PCR was performed with 1X Buffer HF, 0.2 mM dNTP mix, 0.5µM of each primer, 50 ng of gDNA, 3% DMSO and 1 u of Phusion DNA polymerase. The optimum PCR conditions were as indicated in the Table 4.2. Figure 4.1 indicated the schematic representation of construct. First part of the construct was digested with HindIII and EcoRI restriction enzymes and second part of the construct was digested with EcoRI and XbaI restriction enzymes. These constructs were cloned into pcDNA3 plasmid. To do this, pcDNA3 was digested with HindIII and XbaI restriction enzymes. Digested plasmid, first and second parts were mixed within ligation reaction. Ligation mix was transformed into *E.coli* TOP10 competent cells.

Table 4.2. PCR amplification conditions for HBB exon-intron construct.

	Temperature (°C)	Duration	Number of cycles
Initial Denaturation	98	30 sec	1
Denaturation	98	10 sec	35
Annealing	64	30 sec	
Elongation	72	15 sec	
Final Elongation	72	10 min	1

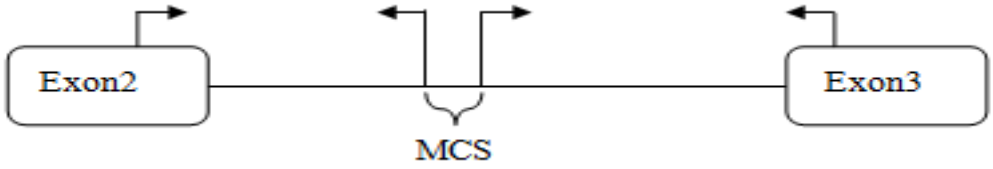

Figure 4.1. Schematic Representation of HBB Exon-Intron Construct.

After *HBB* exon-intron construct was completed with sequence verification, snoRNAs were amplified from gDNA with Phusion High Fidelity DNA Polymerase (Thermo). PCR was performed with 1X Buffer HF, 0.2 mM dNTP mix, 0.5µM of each

primer, 50 ng of gDNA, 3% DMSO and 1 u of Phusion DNA polymerase. For Snord49a, snord49a_fwd_EcoRI and snord49a_rev_BamHI; for Snord65, snord65_fwd_EcoRI and snord65_rev_BamHI primers were used. Amplified snoRNAs and pcDNA3-HBB exon-intron construct plasmid were digested with EcoRI and BamHI. Digested plasmid and snoRNAs were mixed within ligation mix. Ligation mix was transformed into *E.coli* TOP10 competent cells. Figure 4.2 indicated the schematic representation of HBB-SnoRNA construct.

Table 4.3. PCR amplification conditions for snoRNAs.

	Temperature (°C)	Duration	Number of cycles
Initial Denaturation	98	30 sec	1
Denaturation	98	10 sec	35
Annealing	61	30 sec	
Elongation	72	5 sec	
Final Elongation	72	10 min	1

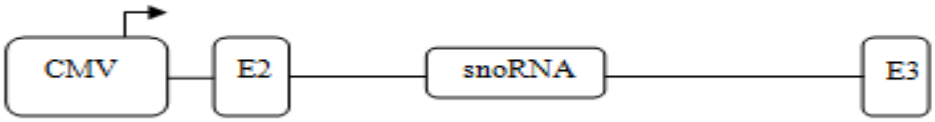

Figure 4.2. Schematic Representation of HBB-SnoRNA Construct.

5. RESULTS

5.1. Bioinformatics Analysis of *C17Orf45* Gene

5.1.1. Phylogenetic Tree for Putative ORF of *C17Orf45* and Its Intronic SnoRNAs

As a first step to analyze *c17orf45* gene, phylogenetic trees were constructed for putative ORF and snoRNAs to examine evolutionary background of the gene. Hence, the nucleotide sequences of putative ORF of *c17orf45* gene were extracted from Blat Search of Genome Browser for different species as indicated in Section 4.1.1. and the sequences were aligned. According to the results, the potential coding region was only observed within primates (Figure 5.1). No homology was observed for other species. Using this alignment file, one of the phylogenetic tree was constructed as mentioned in Section 4.1.2. Second phylogenetic tree was also constructed as following; only nucleotide sequences which were starting with a start codon in the frame till a stop codon were chosen. Hence, this indicated the phylogenetic relationship of the functional part of *c17orf45's* ORF. Phylogenetic trees were as in the Figure 5.2. The results showed that functional part (open reading frame with start and stop codons) indicated a tree like traditional phylogenetic tree. The usage of stop codon moved the gorilla branch close to the ancestral branch. In addition to ORF of the gene, two snoRNAs of *c17orf45* were also analyzed. Extracted data for each snoRNA were aligned (Figure 5.3) and phylogenetic trees were constructed (Figure 5.4).

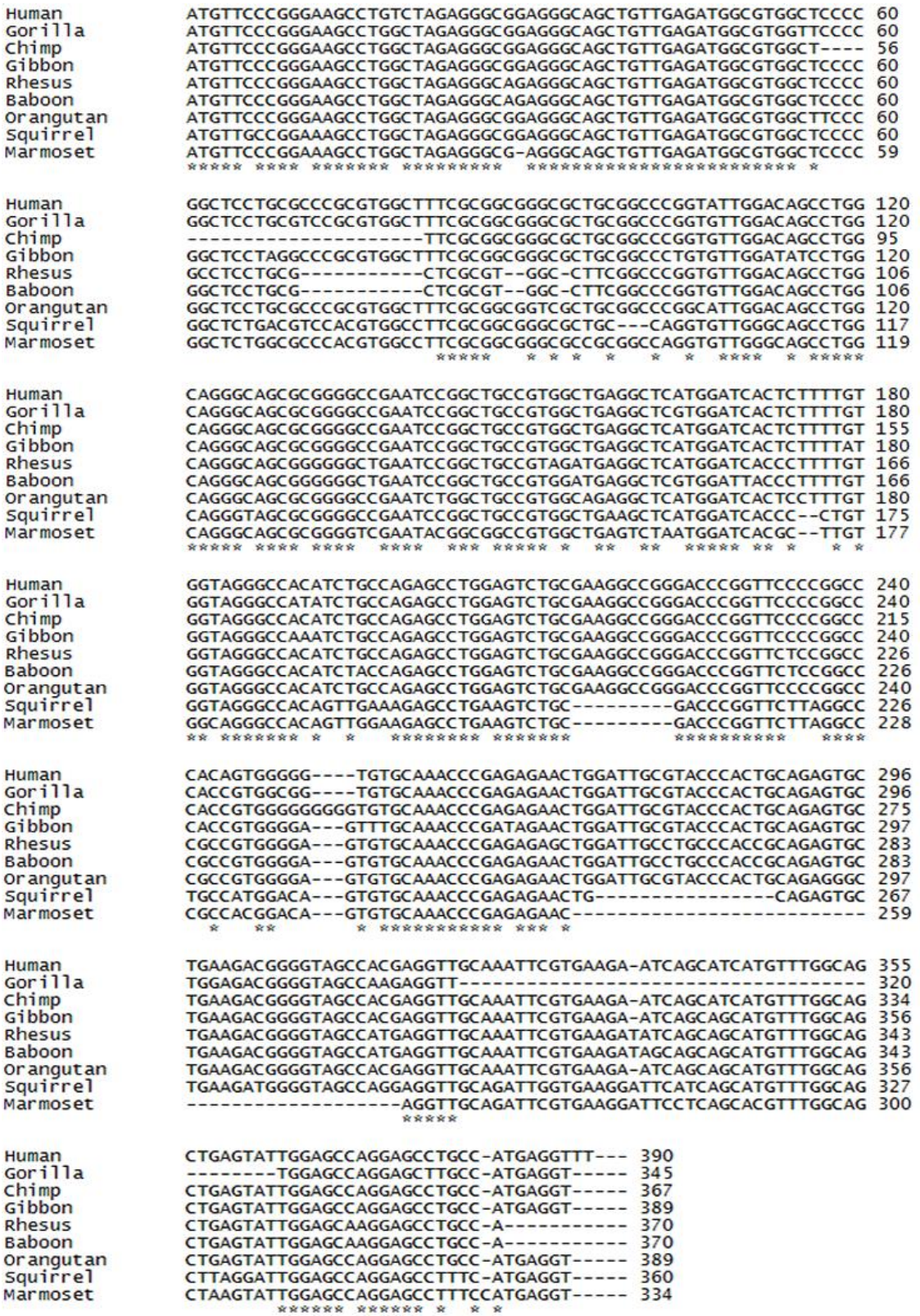

Figure 5.1. Alignment of putative coding regions of *c17orf45* gene among primates.

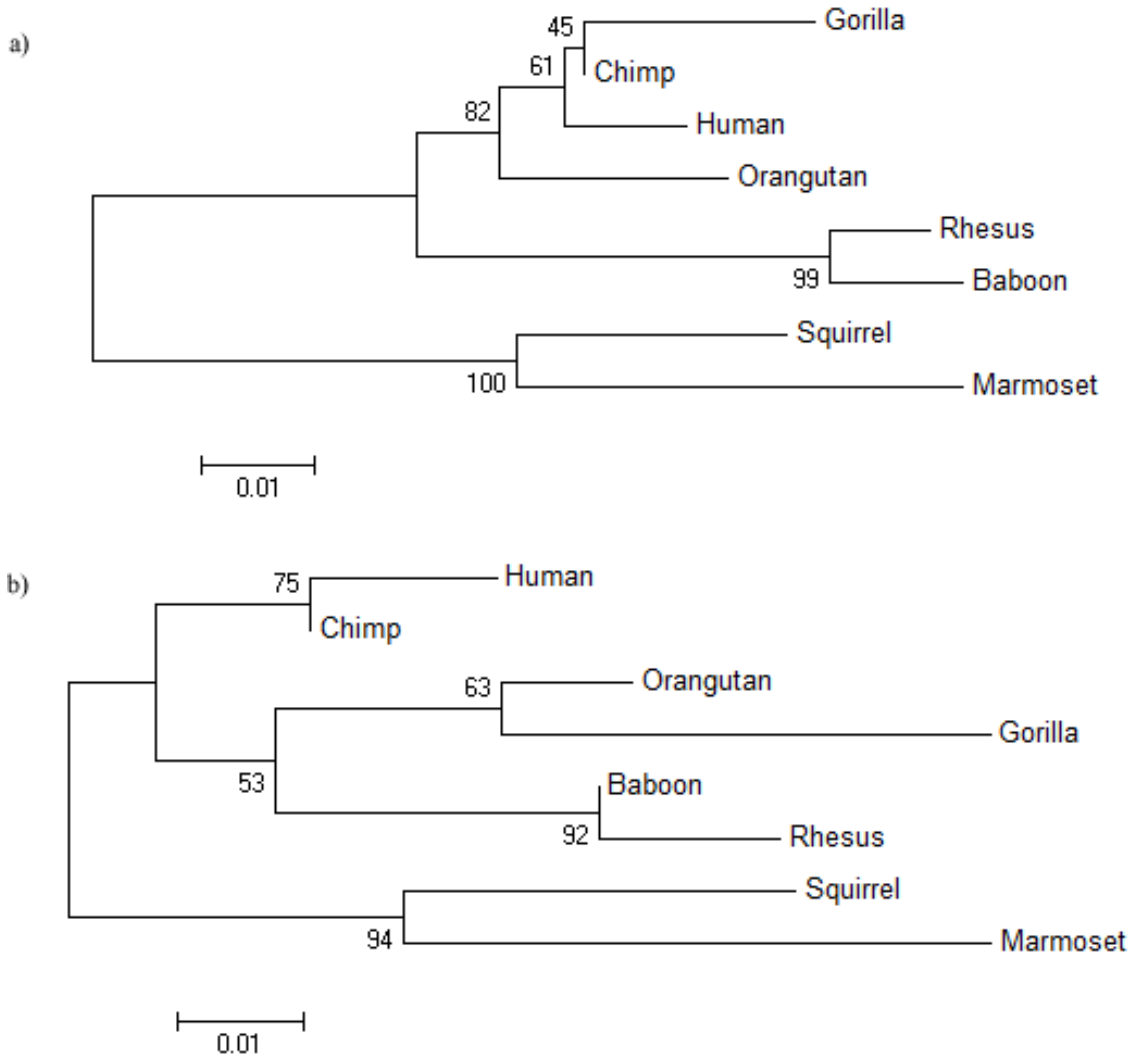

Figure 5.2. Phylogenetic tree for putative *c17orf45* ORF, (a) ORF comparison without considering stop codon and (b) ORF comparison including stop codon (putative functional part).The bootstrap values are indicated on the branches.

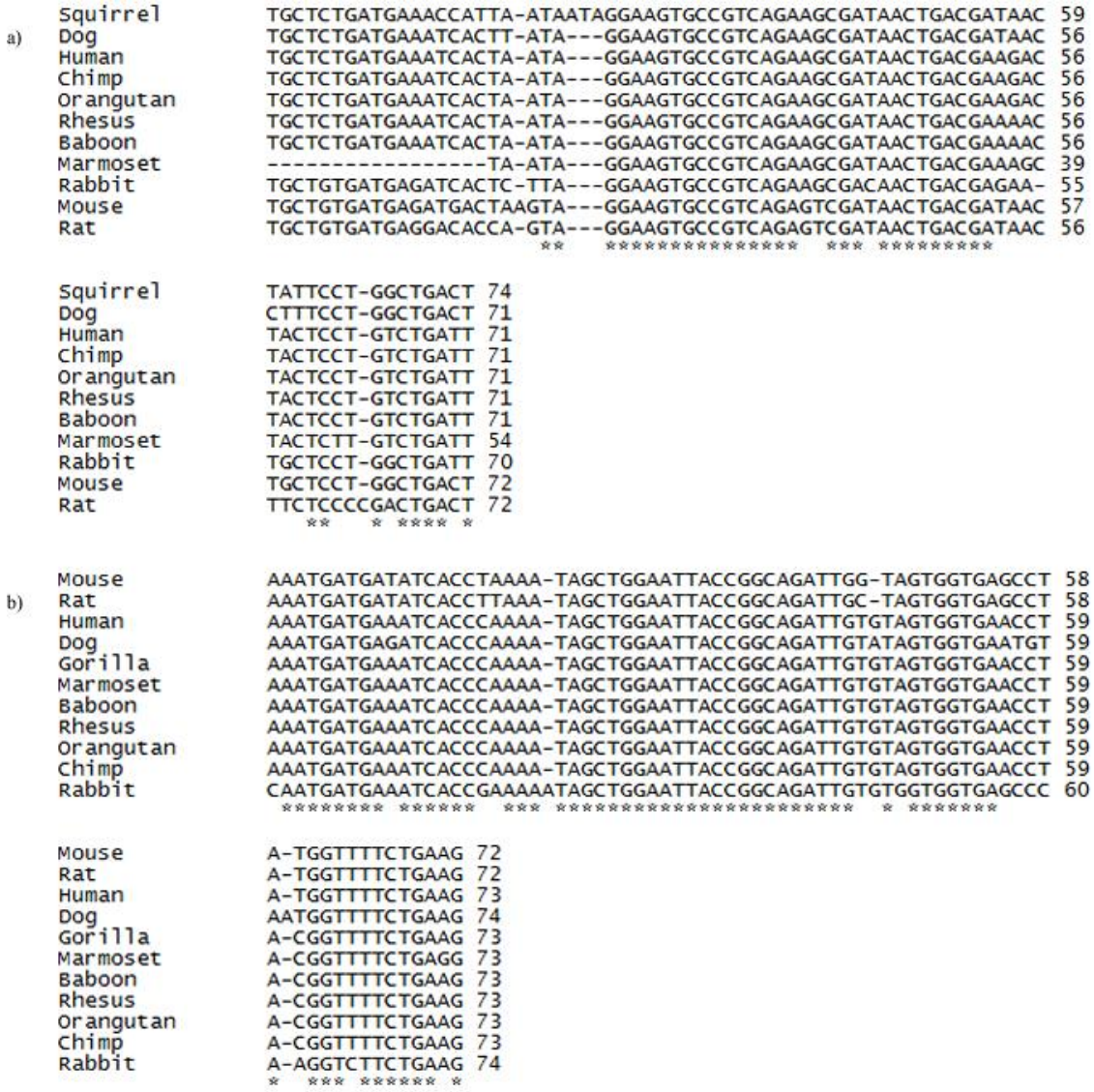

Figure 5.3. Alignment of coding regions of (a) snord49a and (b) snord65 among different vertebrates.

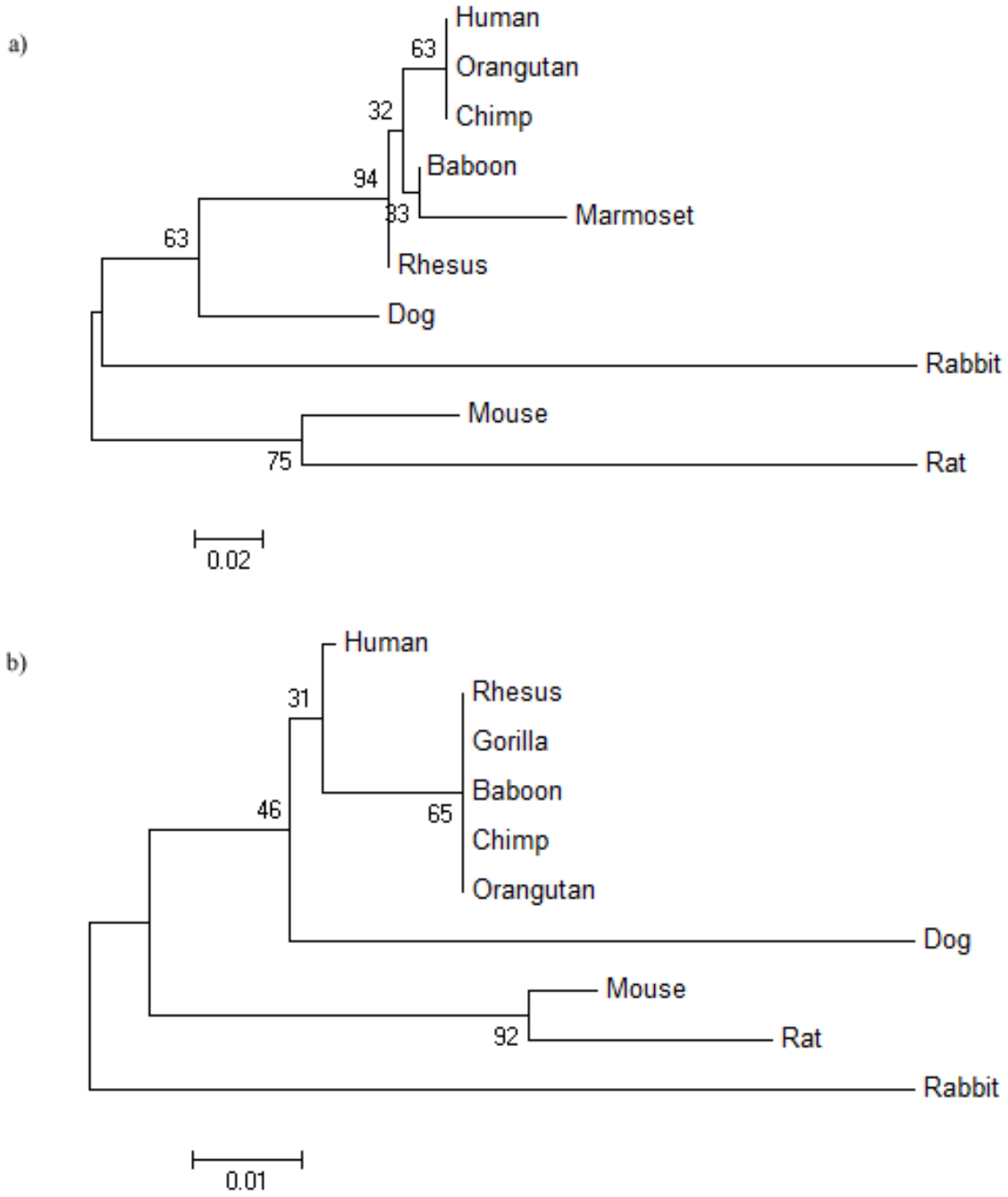

Figure 5.4. Phylogenetic trees for (a) snord49a and (b) snord65.The bootstrap values are indicated on the branches.

5.1.2. Results of PAML Analysis

PAML analysis was performed to discover selective pressure of putative ORF of *c17orf45* gene based on codon substitution by using the ML approach. By means of this analysis, selective pressure on each codon of the gene which may reflect functional properties of the protein could be determined. dN/dS (ω) ratio indicates evolutionary rates on the gene. ω>1 indicates positive selection which means preservation of the beneficial mutations, ω=1 indicates neutral selection expressing the mutations or deletions which have no direct effect on the function of the gene and ω<1 indicates negative (natural) selection which could be explained as the removal of deleterious mutations (Yang, 2007). Three files required for PAML analysis were prepared as in Section 4.1.3. and one ratio model was applied. dN/dS ratio for one ratio model was 1.3855 which indicating a overall positive selection (Nei and Gojobori, 1986). In addition to one ratio model, free ratio model was also applied. Free ratio model provides single dN/dS value for each branch within the tree. However, the free ratio model did not fit dN/dS data significantly (Table 5.1). This might be due to the length of ORF because it was relatively short sequence. On the other hand, the results of the free ratio indicated that there might be a positive selection for putative c17orf45 protein (Figure 5.5) because the values on the branches were pointed out high dN/dS ratios. Especially, the branch between gibbon and orangutan gave high ω value (37.2352) and this case continued till human. Hence, for further analysis, one ratio model was applied with fixed omega values to test the degree of selection. Omega values used in that analysis fixed ranged from 0.1 to 0.5. By doing this, negative (natural) selection would be applied to whole tree; therefore if there was a positive selection on the gene, these omega values implying the negative selection would push the positive selection on the gene more by decreasing the maximum likelihood value. The results indicated that the positive selection persisted till fixed omega value reached to 0.5 which could be accepted as moderate value for negative selection. In addition to this, the statistical test gave significant result for all omega values from 0.1 to 0.5 (Table 5.2); however no significant results were obtained for omega values greater than 0.5. Therefore we conclude that *c17orf45* gene might produce a functional protein.

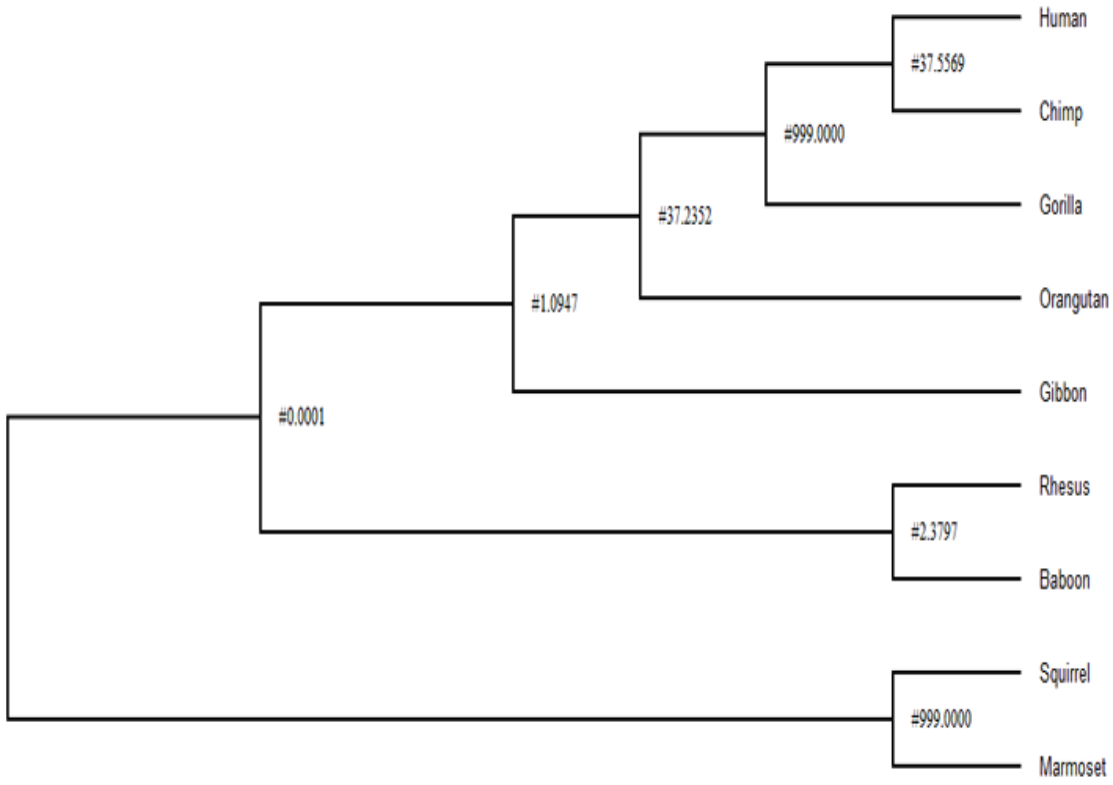

Figure 5.5. Phylogenetic tree after PAML analysis with free ratio model.The values on the branches indicate the ω (dN/dS) ratios.

Table 5.1. PAML analysis results for one and free ratio models(n.s., not significant).

Model	**ω (dN/dS)**	**ln L (the log of maximum likelihood value)**
One ratio model	1,3855	-602,602975
Free ratio model	-	-594,872606
$\chi^2 = 2\Delta \ln L = 15.46$ (dof = 15), n.s.		

Table 5.2. PAML analysis for fixed omega values(** highly significant, p values<0.01; * significant, 0.05<p value<0.01; n.s., not significant).

	ω (dN/dS)	**ln L (the log of maximum likeli-hood value)**	**Degree of freedom**	**χ^2**	
One ratio model	0,1	-643.892102	15	98.04	**
	0,2	-625.401945	15	61.06	**
	0,3	-616.788361	15	43.83	**
	0,4	-611.854481	15	33.96	**
	0,5	-608.74872	15	27.75	*
	0,6	-606.690221	15	23.64	n.s.
Free ratio model	-	-594.872606	-	-	

5.2. Identification of Protein of *C17orf45* Gene

5.2.1. Western Blot for Basal C17orf45 Protein in Different Cell Lines

After obtaining partly promising bioinformatics results about the protein production of the gene, Western Blot experiments were carried out to verify the putative protein of *c17orf45* gene. Therefore, as a first step, basal level of putative c17orf45 protein was searched in different cell lines. Protein lysates were obtained from 10 cm plates or 145 mm plates. The lysates were quantified as indicated in Section 4.2.2. For each lysates, 30 µg of protein were used. Anti-c17orf45 antibody was used to get protein bands. The results showed two different bands for all cell lines except for HEK293FT cell line. One of them was around 70 kDa, the other band was at 35 kDa. The 70 kDa band was probably unspecific. The possible bands for c17orf45 protein were observed around 35 kDa (Figure 5.6) although the theoretical weight of the protein was around 15 kDa.

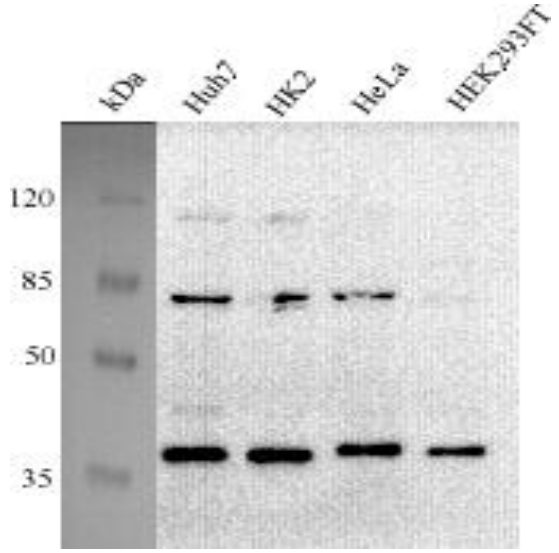

Figure 5.6. Western Blot for c17orf45 protein from different cell lines.

5.2.2. Western Blot for Overexpressed C17orf45 Protein

Following basal protein analysis, overexpression of the gene was performed to observe the increase in the protein level compared to basal level. So, Huh7 cells on 6 well plates were transfected with pcDNA3, pcDNA-c17orf45 and pcDNA-myc-c17orf45 plasmids. Protein lysates were harvested 48 hours after transfection. Collected protein lysates were quantified as mentioned in Section 4.2.2. 30 μg protein lysates were used for each sample. Protein membranes were subjected to anti-c17orf45 and anti-beta actin (loading control) antibodies. The protein bands acquired with anti-c17orf45 were around 35 kDa and the protein bands acquired with anti-beta actin were at 42 kDa. However, there was no difference for the protein level between control and overexpressed samples despite actin levels were similar (Figure 5.7).

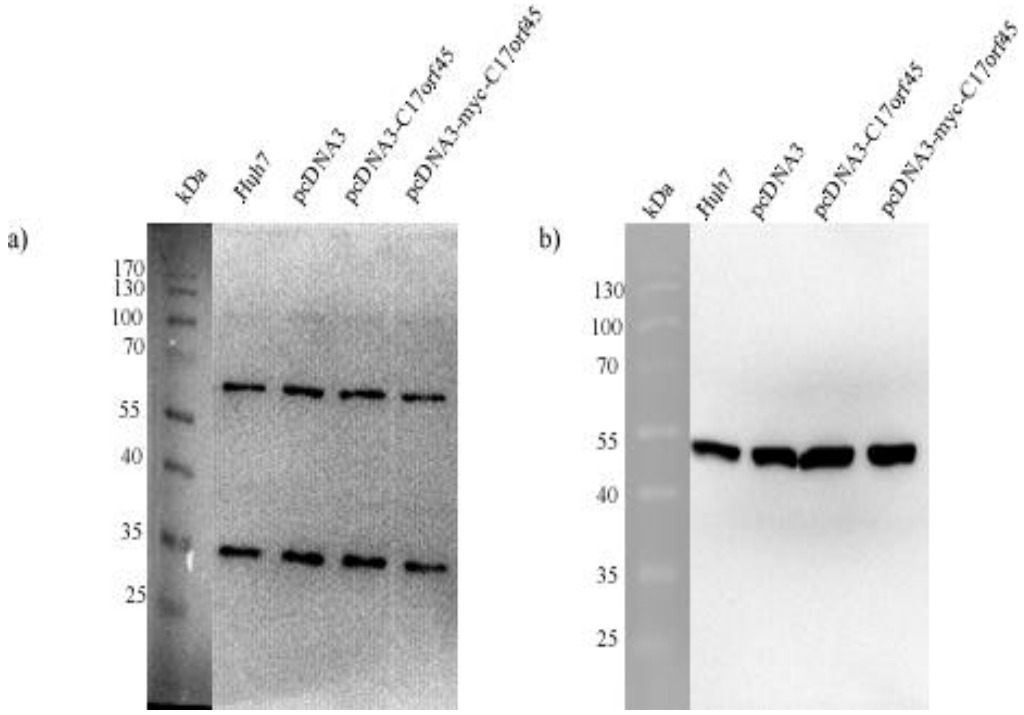

Figure 5.7. Western Blot results for overexpressed c17orf45 protein.Proteins were visualized with (a) anti-c17orf45 and (b) anti-beta actin antibodies.

5.2.3. Western Blot for Tagged C17orf45 Protein

Despite the overexpression analysis, which gave no positive result, tagged c17orf45 constructs were also used to transfect cells in order to compare basal protein and tagged protein levels. Tagged and basal level proteins should indicate the protein bands at same size. Therefore, Huh7 cells on 6 well plate were transfected with pcDNA-c17orf45 and pcDNA-myc-c17orf45 plasmids. Protein lysates were harvested 48 hours after transfection. Obtained protein lysates were quantified as in Section 4.2.2. 30 μg of protein lysates were used for any samples. Collected lysates were subjected to anti-c17orf45, anti-myc antibodies. The protein bands acquired with anti-c17orf45 were around 35 kDa as consistent with previous results; however the protein band acquired with anti-myc antibody was at 26 kDa (Figure 5.8).

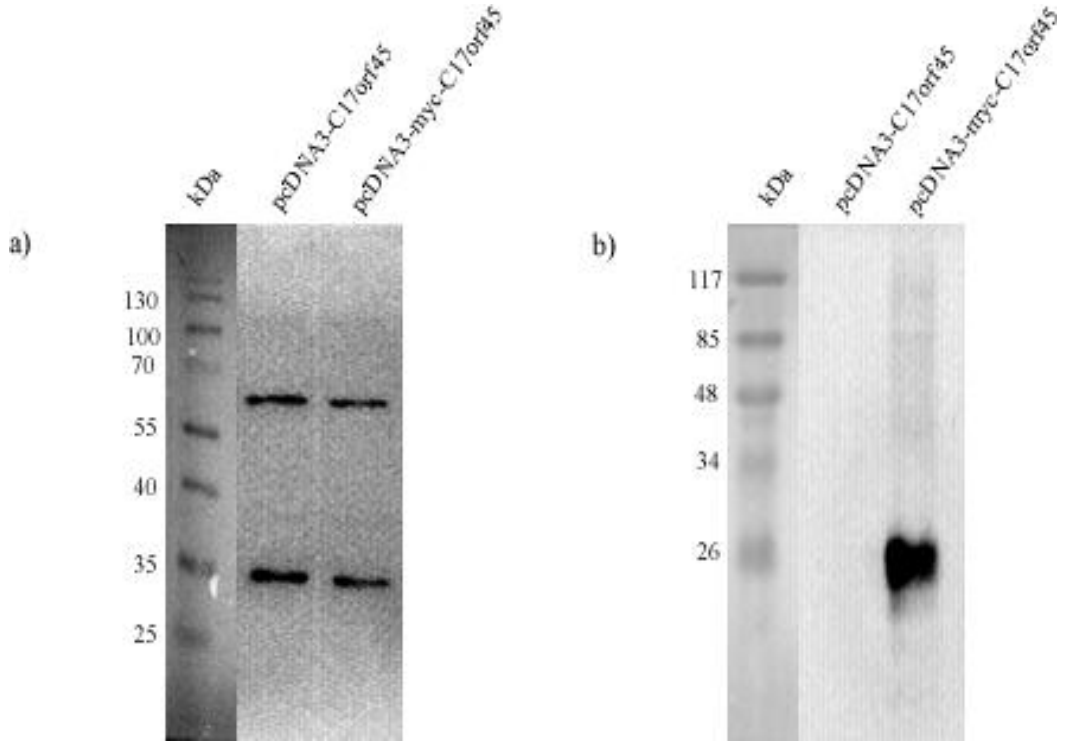

Figure 5.8. Western Blot results for tagged c17orf45 protein.Proteins were visualized with (a) anti-c17orf45 and (b) anti-myc antibodies.

Besides, GFP tagged version of c17orf45 protein was also examined. Because GFP is a relatively large protein (~27 kDa) the shift in the protein band could be easily followed. Therefore, Huh7 cells on 6 well plates were transfected with pIRES2-EGFP and pEGFP-N2-C17orf45 plasmids. Protein lysates were harvested 48 hours after transfection. Concentrations of acquired protein lysates were determined and 30 µg of lysates were used. Collected protein lysates were subjected to anti-c17orf45, anti-GFP antibodies. The protein band obtained via anti-GFP antibody for GFP overexpressed sample was around 27 kDa as expected but there is no band observed for GFP fused c17orf45 protein. In addition to this, when anti-c17orf45 antibody was applied, protein band around 35 kDa was obtained for GFP overexpressed sample which possibly indicating basal level of c17orf45 protein. For GFP fused c17orf45 overexpressed sample, different protein bands were observed. However, it seemed even uppermost band had no possible total mass of fused c17orf45-GFP proteins (Figure 5.9) which should be around 60 kDa theoretically. All of these results suggested that anti-c17orf45 antibody probably did not target putative c17orf45 protein.

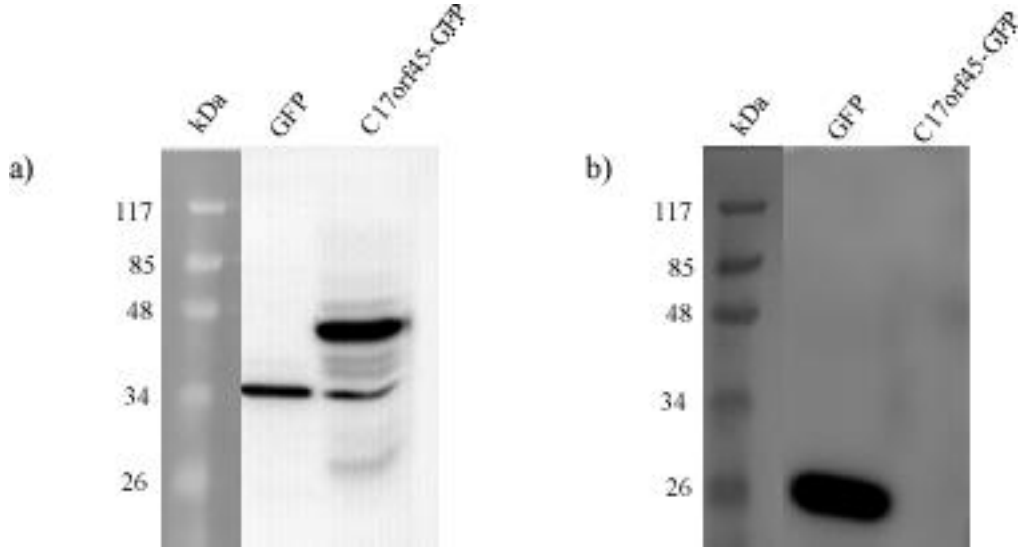

Figure 5.9. Western Blot results for tagged c17orf45 protein.Proteins were visualized with (a) anti-c17orf45 and (b) anti-GFP antibodies.

5.2.4. Western Blot for Immunoprecipitated C17orf45 Protein

Previous protein analysis results were the indicator that anti-c17orf45 antibody did not recognize the expected protein. Immunoprecipitation was performed to verify further that the antibody did not identify the protein and to know which protein was recognized by the antibody. For this purpose, pure protein band (35 kDa) could be obtained and it could be sequenced. Hence, Huh7 cells on 10 cm plate were harvested with lysis buffer. Protein was quantified and 500 µg of Huh7 protein lysate was immunoprecipitated with anti-c17orf45 antibody. Immunoprecipitation protocol was as mentioned in Section 4.2.4. Immunoprecipitated proteins were subjected to Western Blot and visualized with anti-c17orf45 antibody. As indicated in the protocol part, supernatant and 1st wash liquids were collected as control. The protein band attained with anti-c17orf45 after immunoprecipitation was around 35 kDa as expected (Figure 5.10).

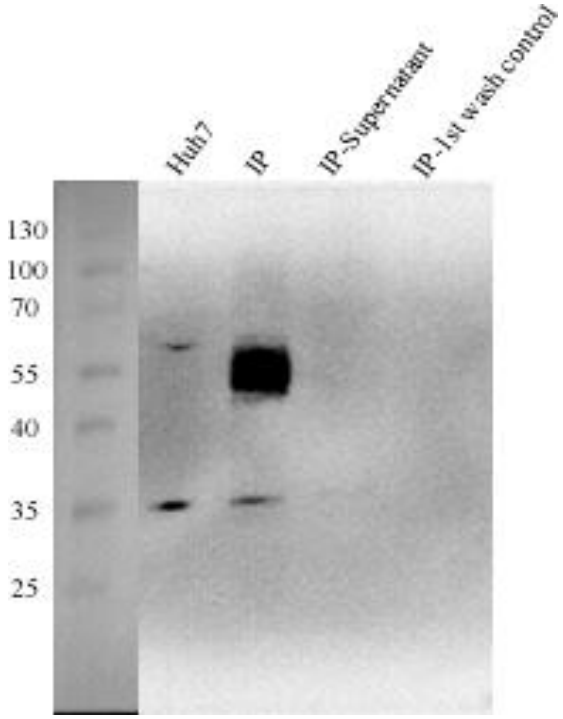

Figure 5.10. Western Blot results for immunoprecipitated c17orf45 protein.

5.2.5. Coomassie Blue Staining for Immunoprecipitated C17orf45 Protein

Immunoprecipitation followed by Western Blot indicated that pure protein was perfectly obtained. To get protein band to sequence it, SDS-PAGE gel was stained with Coomassie Blue. The immunoprecipitated protein lysate was loaded into SDS-PAGE and after running, staining procedure was applied as indicated in Section 4.2.7. Stained protein sample gave a band around 35 kDa as shown in Figure 5.11.

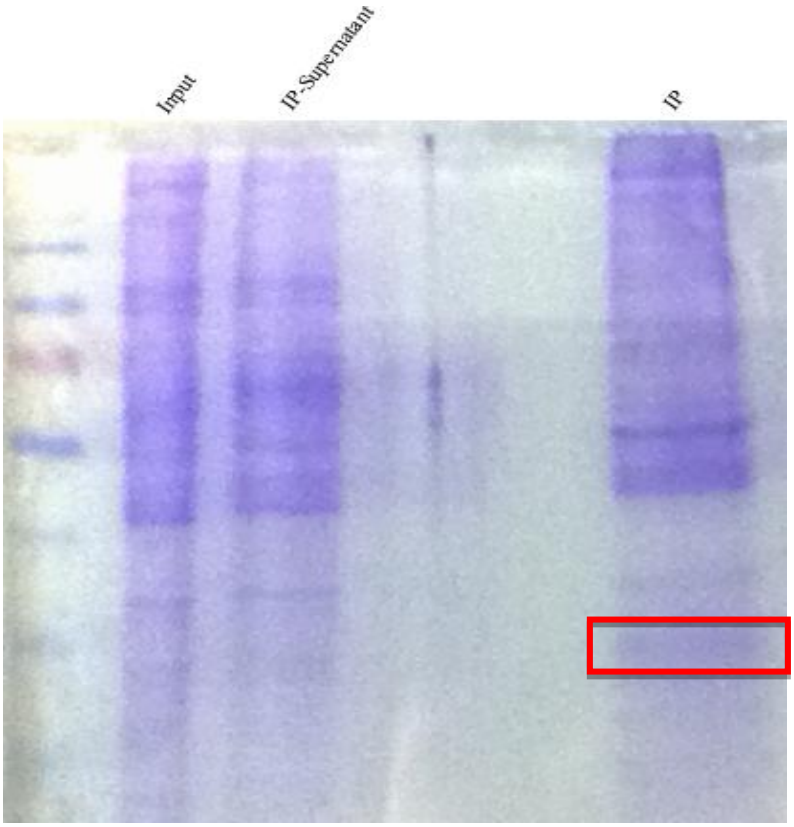

Figure 5.11. Coomassie Blue Staining for immunoprecipitated c17orf45 protein.

5.2.6. Mass Spectrometry Results for C17orf45 Protein

To send the pure protein for sequencing, the protein band stained with Coomassie Blue was cut with razor blade and placed into 1.5 ml micro centrifuge tube. Sample was directly sent to the mass spectrometry analysis center. Mass spectrometry was performed to acquire the amino acid sequence of any proteins. The result of mass spectrometry analysis showed that protein for *c17orf45* gene was not suggested among the possible proteins recognized by anti-c17orf45 (Table 5.3). Instead of c17orf45 protein, other proteins like ribosomal proteins were possible targeted by anti-c17orf45 antibody.

Table 5.3. Results of Mass Spectrometry Analysis of Putative C17orf45 Protein.

	Gene Symbol	Name	Swiss Prot. Accession Number	Mass	Start-Finish	Score
1	RS6	40S ribosomal protein S6	P62753	28663	32 – 46	83
					32 – 46	69
					120 – 131	34
2	RS3	40S ribosomal protein S3	P23396	29926	28 – 40	46
					77 – 90	36
					19 – 27	20
					46 – 54	8
3	RS2	40S ribosomal protein S2	P15880	31305	213 – 227	18
					77 – 89	71
4	SRFS1	Serine/arginine-rich splicing factor 1	Q07955	27728	123 – 138	50
					18 – 28	40
5	RS3A	40S ribosomal protein S3a	P61247	29926	66 – 82	83
6	RACK1	Guanine nucleotide-binding protein subunit beta-2-like 1	Q6FH47	35055	89 – 99	39
7	RL7A	60S ribosomal protein L7a	P62424	29977	38 – 48	8
8	EF1B	Elongation factor 1-beta	P24534	24748	8 – 22	32
9	PHB2	Prohibitin-2	Q99623	33276	271 – 289	14
10	H15	Histone H1.5	P16401	22566	38 – 49	20
11	RAB18	Ras-related protein Rab-18	Q9NP72	22963	113 – 123	4
12	PERP1	Plasma cell-induced resident endoplasmic reticulum protein	Q8WU39	20681	81 – 93	6

5.3. HBB-SnoRNA Construct Design

Apart from protein analysis, snoRNAs of *c17orf45* gene were examined. Intronic snoRNAs (snord49a and snord65) of *c17orf45* gene were cloned into intron of *beta-globin* gene residing between two sequential exons. By doing this, the splicing which was the first step of obtaining functional snoRNA *in vitro* could be managed. Then, it would help to examine whether these snoRNAs had any impacts on cell cycle in different cancer cell lines. Cloning strategy was mentioned in Section 4.5.

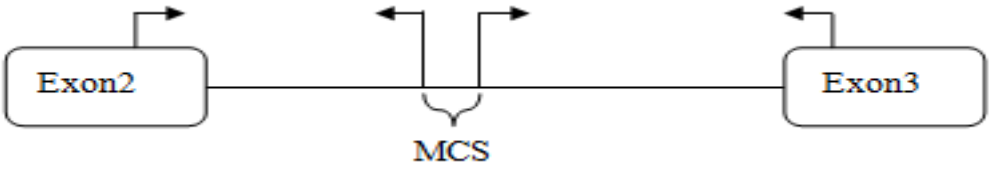

Figure 5.12. Representation of HBB-snoRNA cloning strategy.

First of all, exon2-intron2 part of the construct and intron2-exon3 part of the construct which were around 450 bp were amplified from genomic DNA and run in 1% agarose gel (Figure 5.13).

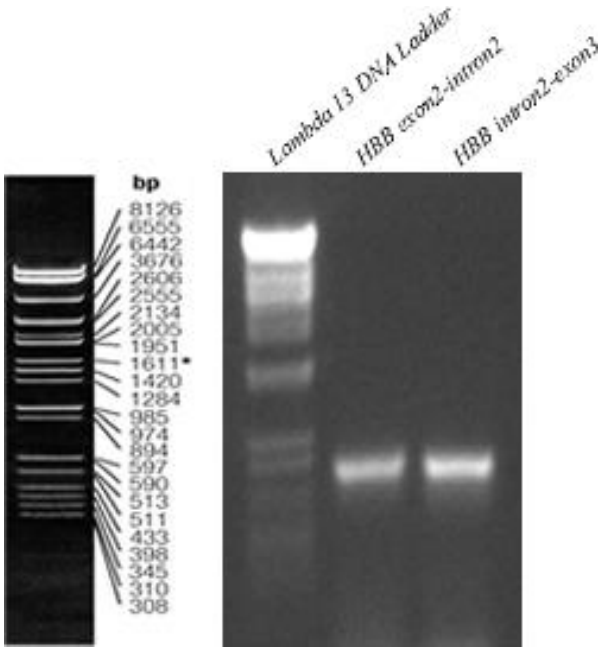

Figure 5.13. PCR amplification of HBB exon2-intron2 and intron2-exon3.

After amplification, PCR purification was applied to the fragments. Fragments were digested with HindIII-EcoRI and EcoRI-XbaI restriction enzymes, respectively. pcDNA3 plasmid was also digested with HindIII-XbaI restriction enzymes. Two fragments and plasmid were ligated and transformed into bacteria. Colony PCR was applied to the colonies to obtain plasmid containing ligated fragments. Positive colonies were selected and verified via sequencing. Therefore, two exonic part and the whole intron among them were perfectly obtained and called pcDNA3-HBB. Besides, intronic part

provided a multiple cloning site (MCS) apart from MCS of plasmid. So, snoRNAs amplified from genomic DNA (Figure 5.14) could be cloned to MCS of the construct.

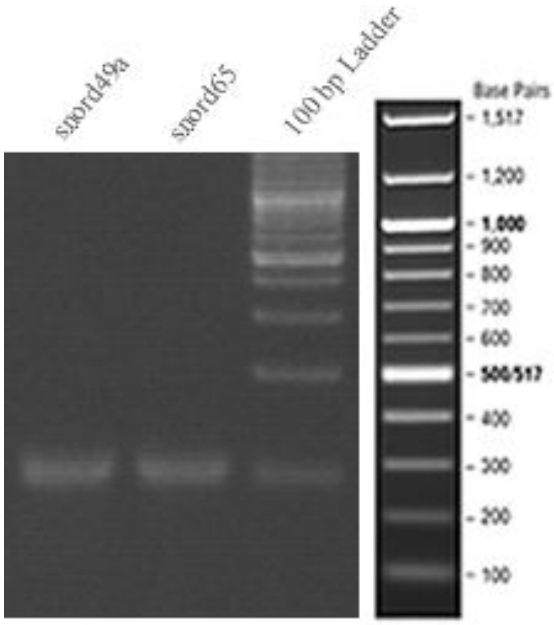

Figure 5.14. PCR amplification of snord49a and snord65 from gDNA.

Amplified snoRNAs were purified and then, digested with EcoRI-BamHI restriction enzymes. pcDNA3-HBB plasmid was also digested with the same restriction enzymes. Digested snoRNAs and pcDNA3-HBB were ligated and transformed into bacteria. Colony PCR was performed and positive colonies were chosen. Plasmids containing snoRNAs were purified and PCR was performed with the primers on the plasmid (universal primers; SP6 and T7) to indicate snoRNA containing plasmid (Figure 5.15). Sequencing was done to verify the correct sequences of final constructs. The final constructs were named as pcDNA3-HBB-snord49a and pcDNA3-HBB-snord65.

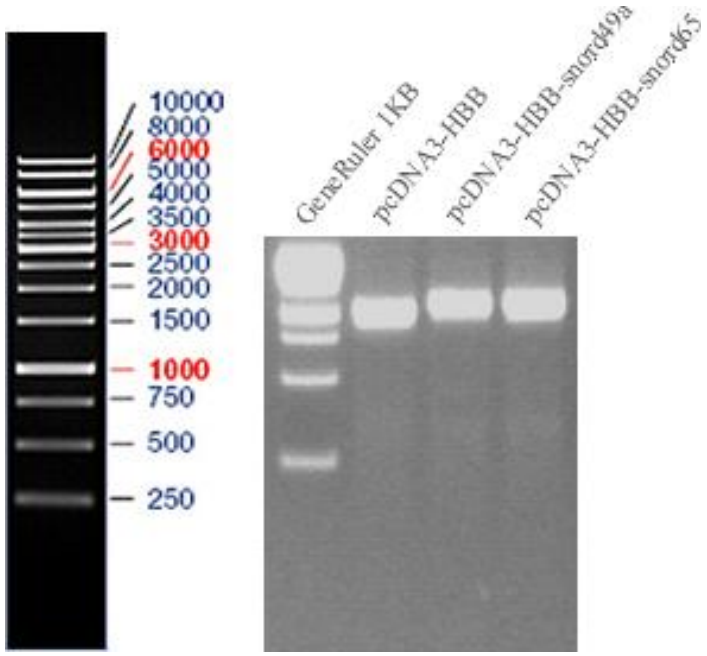

Figure 5.15. PCR analysis for pcDNA3-HBB and pcDNA3-HBB-snoRNAs.

5.4. Verification of Splicing in HBB-snoRNA Constructs

5.4.1. RT-PCR Results of HBB-snoRNA Constructs

After successfully cloning the HBB-snoRNA construct, splicing of exons were tested. One of these tests was done with RT-PCR. By RT-PCR, overexpression of spliced version of constructs compared to basal level could be seen on agarose gel. So, Huh7 cells on 6 well plates were transfected with pcDNA3, pcDNA3-HBB-snord49a and pcDNA3-HBB-snord65 plasmids. 48 hours after tranfection, RNA isolation was performed to cells containing plasmids as indicated in Section 4.3.9. cDNA synthesis was performed with RNA samples as indicated in Section 4.3.10. cDNAs were used in RT-PCR analysis for verification of splicing. As indicated in the Figure 5.16, spliced version of samples was observed around 70 bp as expected. Interestingly, pcDNA3 samples indicating basal level of spliced *beta-globin* RNA had slightly lower band compared to samples including snoRNAs. Besides, genomic DNA indicated a band around 1000 bp as expected. For pcDNA3-HBB-snord49a sample, an unspecific band was observed around 200 bp.

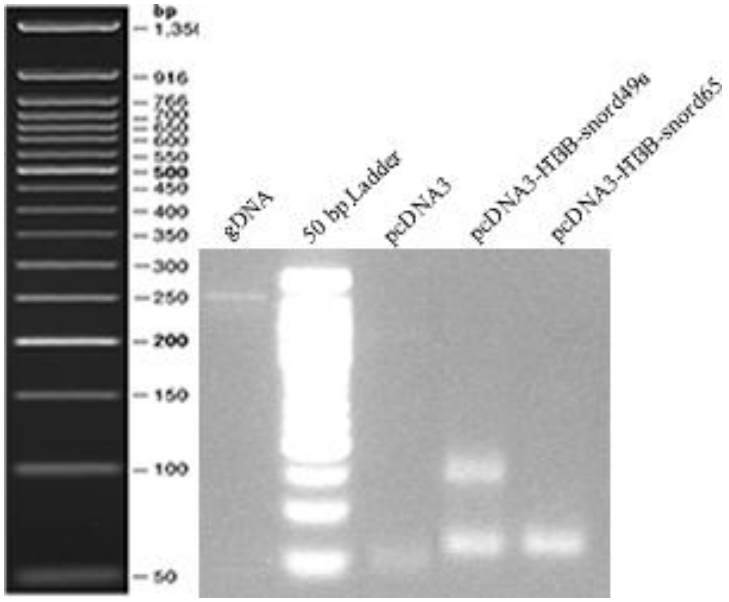

Figure 5.16. RT-PCR analysis for HBB-snoRNA splicing.

Another run of RT-PCR for *beta-globin* constructs was performed to verify splicing. RNA samples were run with HBB primers and GAPDH (loading control) primers. Overexpression of spliced versions of constructs compared to control sample was observed (Figure 5.17). These RT-PCR results indicated that splicing of the construct worked well.

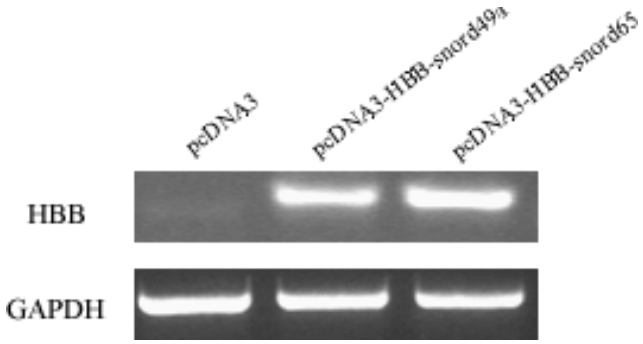

Figure 5.17. RT-PCR analysis indicating overexpression of spliced constructs.GAPDH was used for loading control.

RT-PCR analysis was also performed to check overexpression of snoRNAs. For snord49a, SNORD49A_fwd_EcoRI and SNORD49A_rev_BamHI primers were used. For snord65, SNORD65_fwd_EcoRI and SNORD65_rev_BamHI primers were used.

Overexpressed samples indicated brighter bands and snoRNAs were observed around 100 bp as expected (Figure 5.18). This could also be accepted that overexpression of snoRNAs was the indication of splicing; however this might result from overexpression from pre-mRNA instead of spliced out intron.

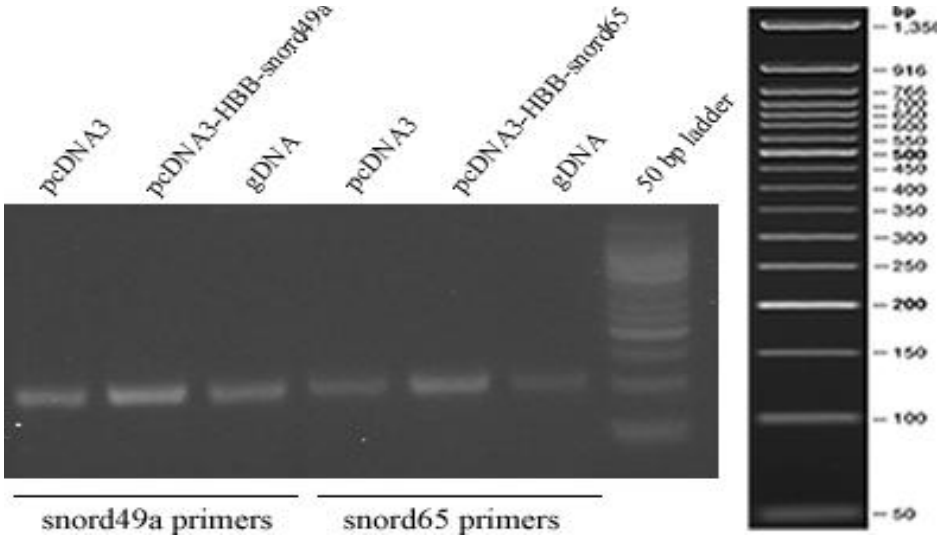

Figure 5.18. RT-PCR analysis indicating snord49a and snord65 overexpression.

5.4.2. Real Time PCR Results of HBB-snoRNA Constructs

Real Time PCR analysis was performed for *HBB* constructs both to verify the splicing and to quantitate the overexpression level. Short elongation time during PCR would probably provide the amplification of spliced exons of *HBB* gene. In other words, if splicing did not occur, the overexpression of samples might not be observed. Real Time PCR was performed as indicated in Section 4.3.12. cDNAs of constructs were amplified with HBB_spliced_RT_Fwd and HBB_spliced_RT_Rev primers for *HBB* constructs, SNORD49A_fwd_EcoRI and SNORD49A_rev_BamHI for snord49a, SNORD65_fwd_EcoRI and SNORD65_rev_BamHI for snord65 samples. Normalization was done according to 18S and SDHA genes (Figure 5.19).

a)

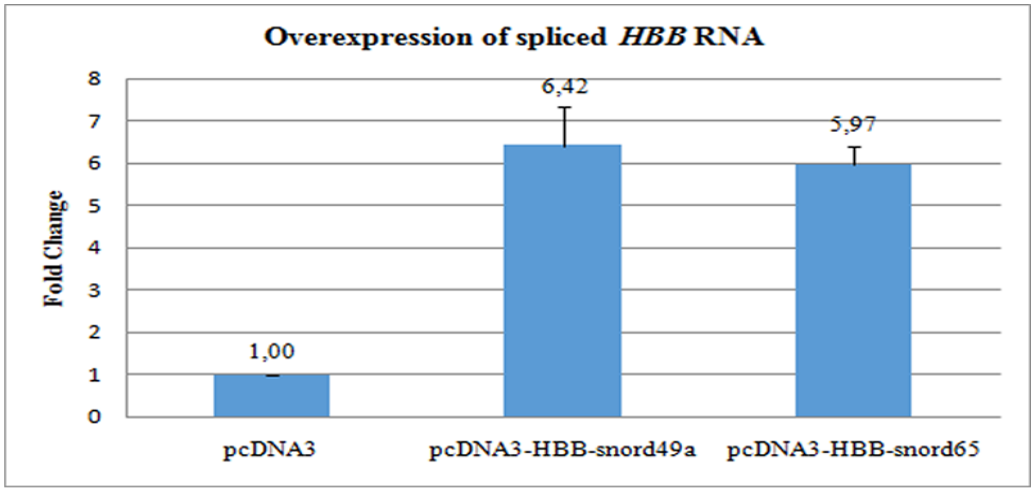

b)

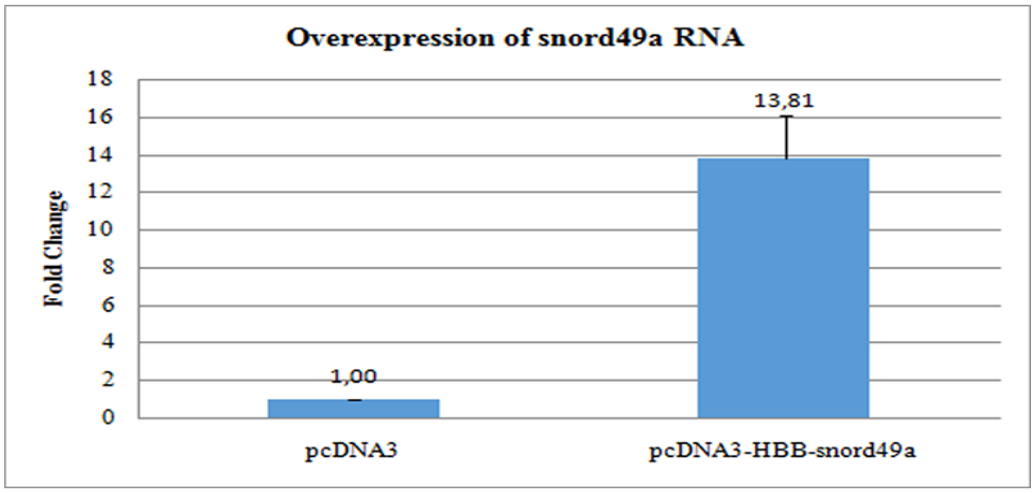

c)

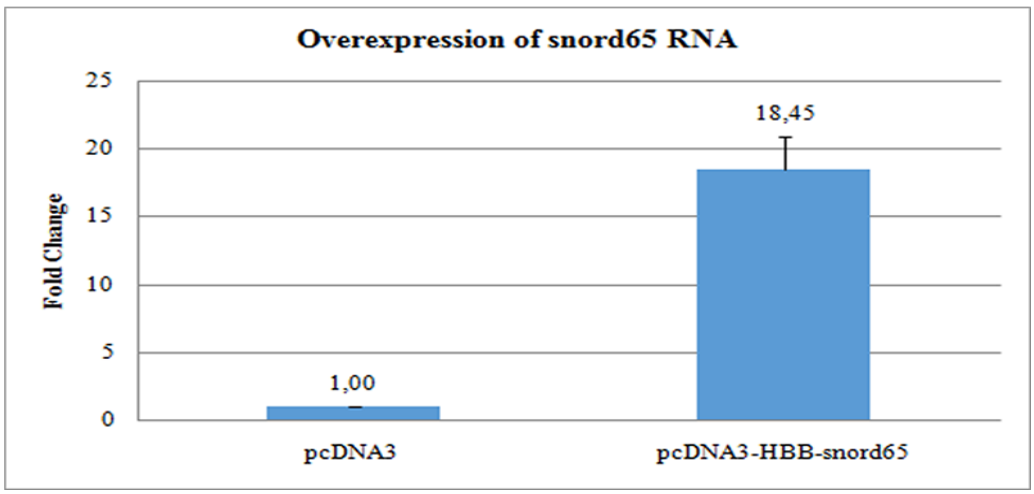

Figure 5.19. Real Time PCR results for (a) spliced *HBB* RNAs overexpression, (b) snord49a RNA overexpression and (c) snord65 RNA overexpression.The graphs indicate the results of two independent experiments.

The results of Real Time PCR showed that splicing machinery worked and over-expression was seen as 6.42 and 5.97 fold for pcDNA3-HBB-snord49a and pcDNA3-HBB-snord65 samples with HBB primers (splicing primers), respectively. When analysis was done with snoRNA primers, overexpression was observed as 13.81 fold for pcDNA3-HBB-snord49a and 18.45 fold for pcDNA3-HBB-snord65.

5.4.3. Fluorescent Microscopy Results for YFP-fused HBB Peptide

To further validate that splicing machinery worked for these constructs, pcDNA3-HBB-snord49a and pcDNA3-HBB-snord65 plasmids were used to constitute YFP fused *beta-globin* protein. By these amplifications, exons of *HBB* were made in-frame of YFP protein. In other words, if splicing happened, YFP fused HBB protein would be obtained. To do this, PCR amplification was performed to pcDNA3-HBB-snord49a and pcDNA3-HBB-snord65 with HBB_e2fwd_GFP_Bgl2 and HBB_e3rev_GFP_Hind3 primers. Then, amplified PCR fragments and pEYFP-N1 plasmid were digested with BglII and HindIII restriction enzymes. Digested products were purified and ligation was performed. Ligation mix was transformed into bacterial cells and positive colonies were chosen via colony PCR. After sequence verification, Huh7 cells were transfected either with pEYFP-N1-HBB-snord49a or pEYFP-N1-HBB-snord65. 48 hours after transfection, cells were examined under fluorescent microscopy with 10X objectives (Figure 5.20).

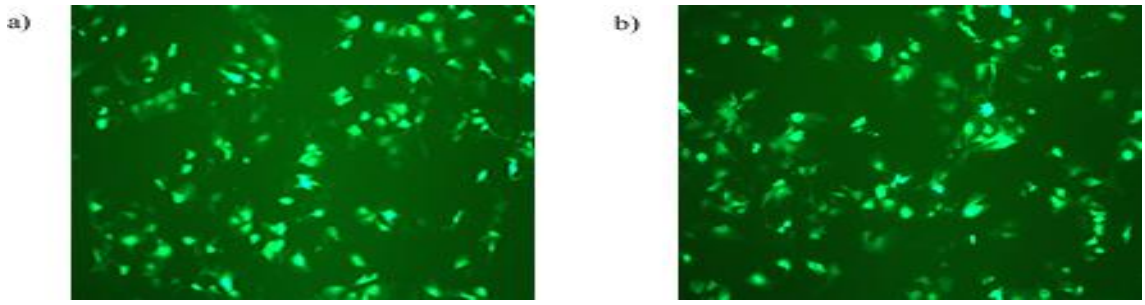

Figure 5.20. Fluorescent microscopy images for (a) pEYFP-N1-HBB-snord49a and (b) pEYFP-N1-HBB-snord65.

The fluorescent microscopy results suggested that the intron between exons were removed via splicing. Spliced exons joined together and constitute fused YFP protein. All of these results showed that splicing occured successfully for both HBB-snoRNA constructs.

5.5. Cell Cycle Analysis

After it was determined that splicing was successful for HBB-snoRNA constructs, these constructs were used to analyze whether snoRNAs of *c17orf45* gene had any specific impacts on cell cycle stages in different cancerous cell lines. To do this, 5 different cell lines which were HEK293FT, HeLa, Huh7, U373-MG and MCF-7 were utilized. 2 different time points (24 or 48 hours after transfection) were applied. The criterion in the determination of time points was the duplication time of each cell line. Because HEK293FT and HeLa cell lines duplicated fast compared to other cell lines used in this study, these cell lines were analyzed 24 hours after transfection. Other cell lines except MCF-7, which was examined only for 24 hours, were analyzed both for 24 and 48 hours. Cell cycle analysis was performed as indicated in Section 4.3.13. Briefly, procedure was started with the transfection of cells with either pcDNA3-HBB, pcDNA3-HBB-snord49a or pcDNA3-HBB-snord65 plasmids. According to time points, 24 or 48 hours after transfection, media of cells were collected to observe any apoptotic cells. Cells were washed and 70% ethanol was added and incubated on ice for 2 hours. After washing cells, 1 ml of PI stain containing RNAse A was added onto cells and incubated at 37°C for 45 minutes. Then, cells were washed, resuspended in 1X PBS and analyzed in FACSCalibur machine.

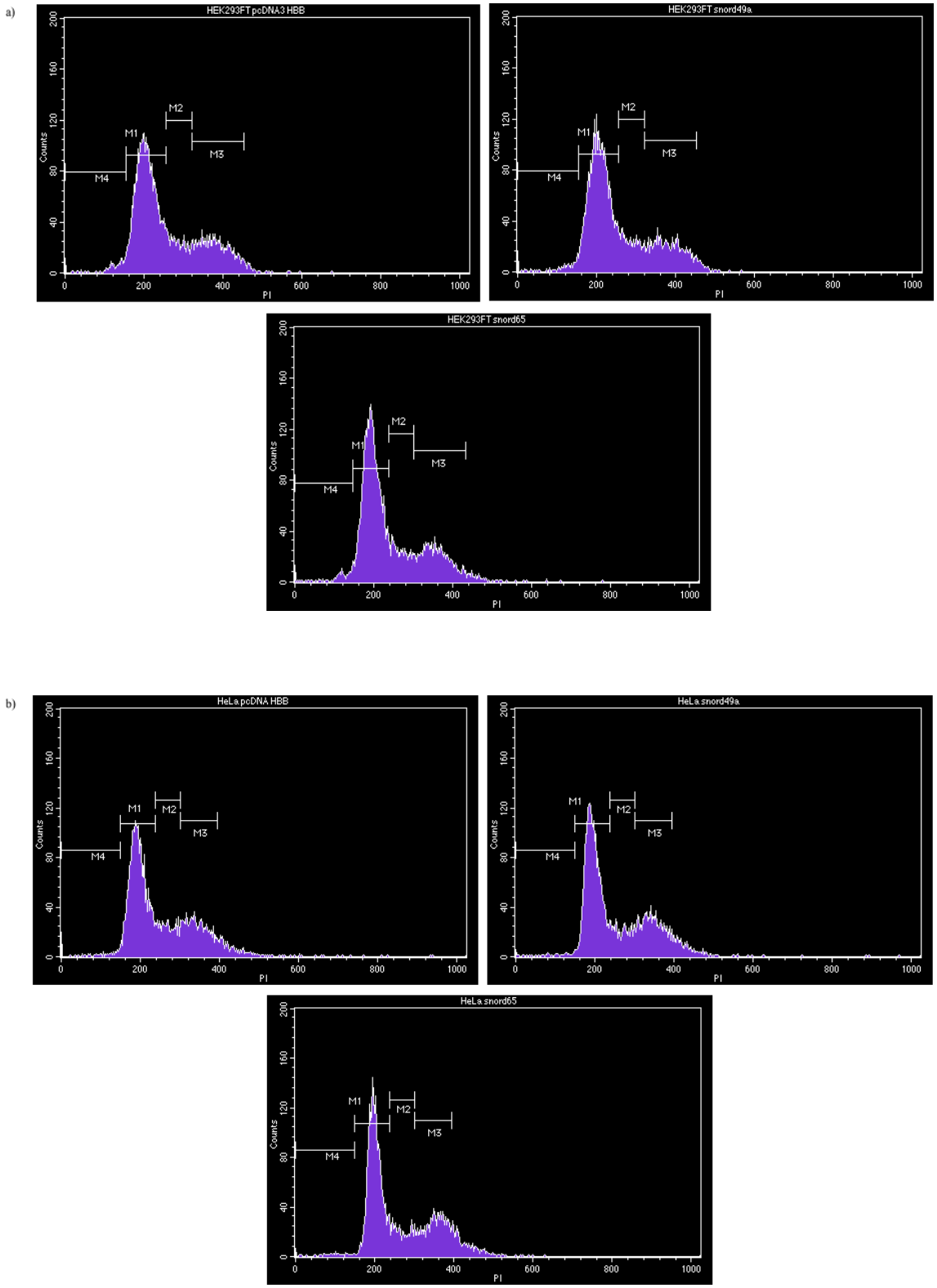

Figure 5.21. Cell cycle analysis for different cell lines. (a) HEK293FT 24h, (b) HeLa 24h. Stages indicated with M4,M1,M2 and M3 corresponded to sub-G1, G1, S and G2, respectively.

The results of the cell cycle analysis for HEK293FT and HeLa cells indicated that there was no significant difference among control and experimental groups for both cell lines (Figure 5.21, a and b). HEK293FT cell line was used as non-cancerous cell line which could be accepted as the control cell line. Because it was speculated that these snoRNAs might affect cancer cells, it was expected that there might not be any difference within control and samples in HEK293FT cell. However, there were not any changes on cell cycle stages of HeLa cell line, too.

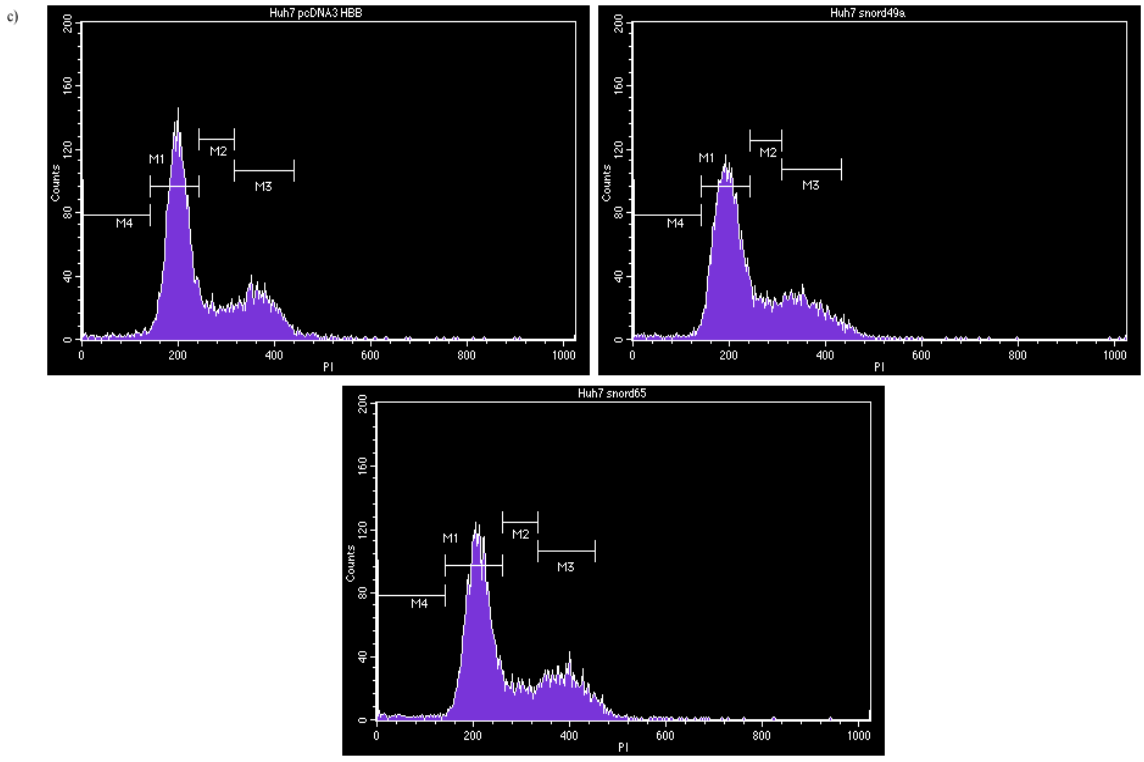

Figure 5.20. Cell cycle analysis for different cell lines (cont.). (c) Huh7 24h. Stages indicated with M4,M1,M2 and M3 corresponded to sub-G1, G1, S and G2, respectively.

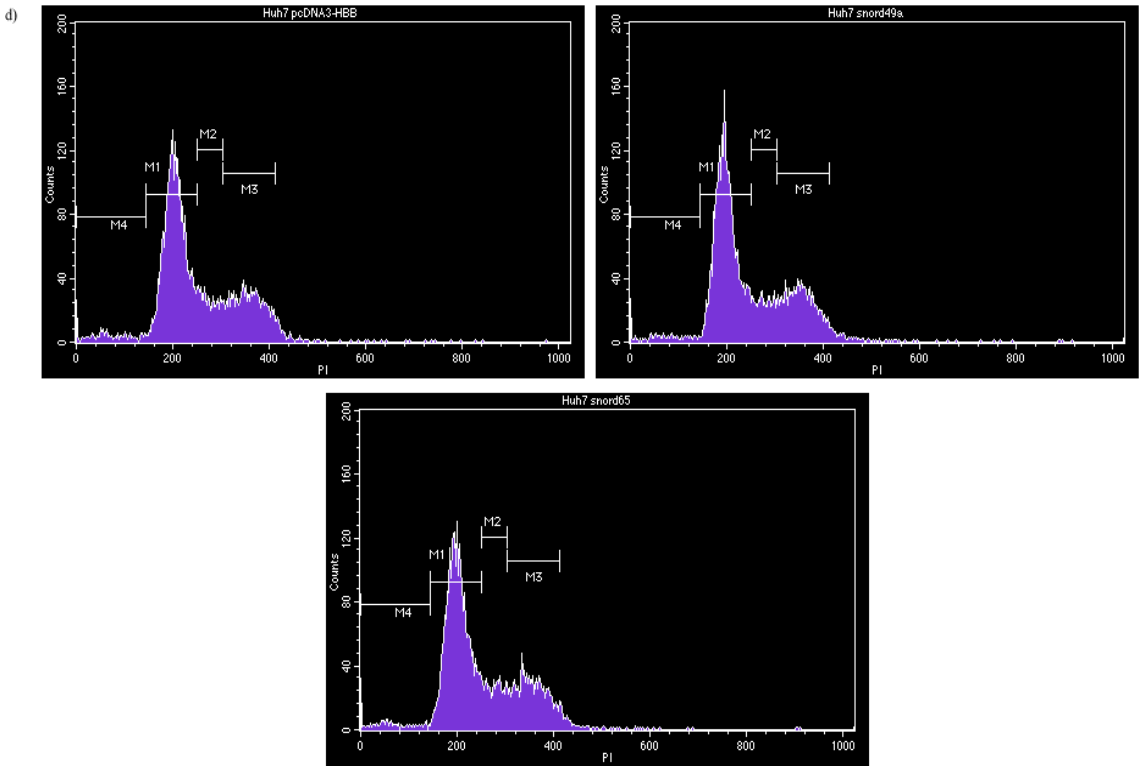

Figure 5.20. Cell cycle analysis for different cell lines (cont.). (d) Huh7 48h. Stages indicated with M4,M1,M2 and M3 corresponded to sub-G1, G1, S and G2, respectively.

Similarly, Huh7 cell line, which was a hepatocellular carcinoma cell line, did not indicate any variations among samples for two time points (Figure 5.21, c and d). The percentages of each cell cycle stage showed very close and like results. In a similar content, U373-MG, human astrocytoma cell line, revealed no alteration as Huh7 and HeLa cell lines (Figure 5.21, e and f). In addition, there were many dead cells for all samples at 48 hours for U373-MG cell line (Table 5.4). It was also observed under bright field microscopy. This might result from the toxic effect of transfection to the cell.

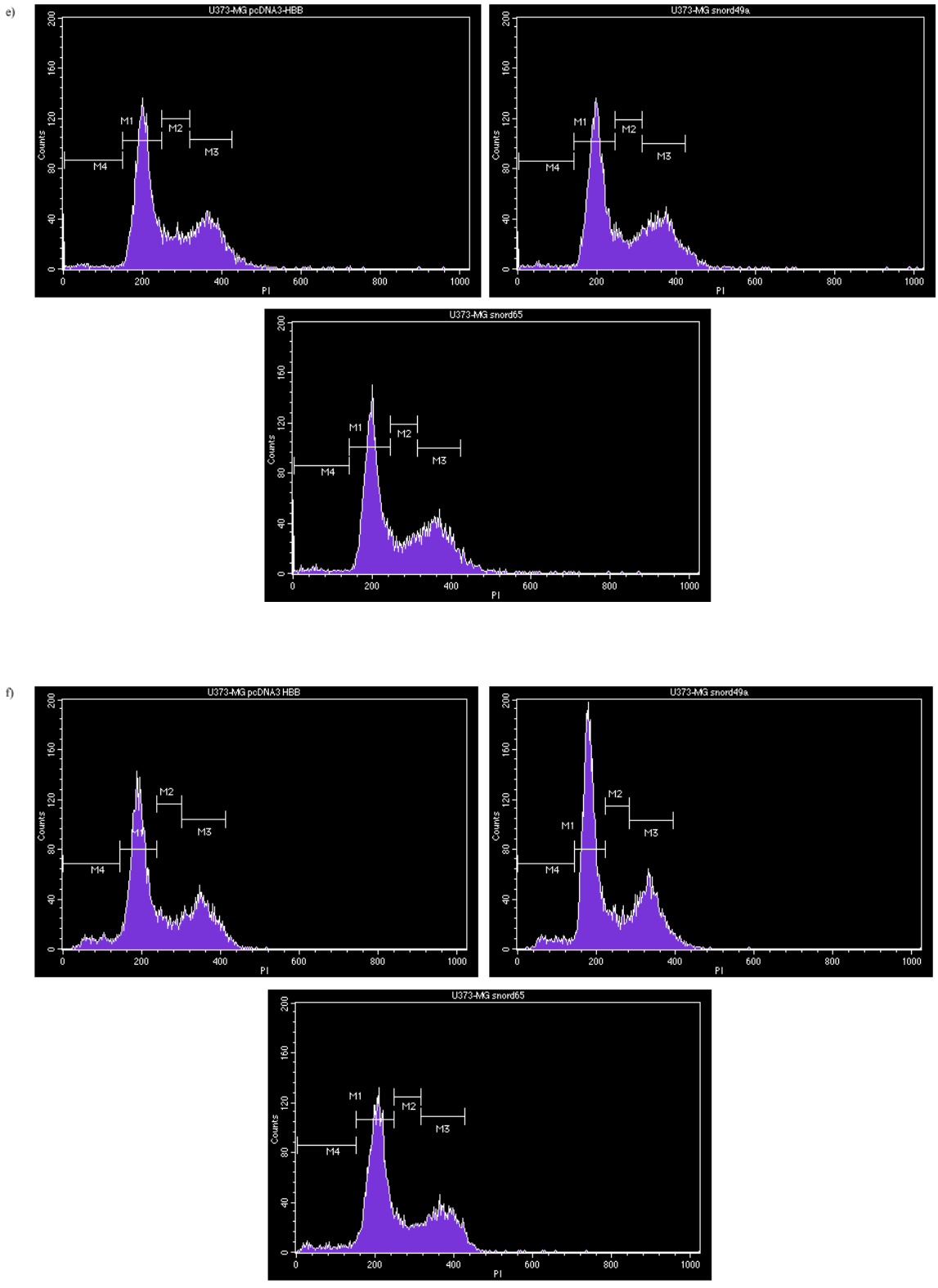

Figure 5.20. Cell cycle analysis for different cell lines (cont.). (e) U373-MG 24h, (f) U373-MG 48h. Stages indicated with M4,M1,M2 and M3 corresponded to sub-G1, G1, S and G2, respectively.

g)

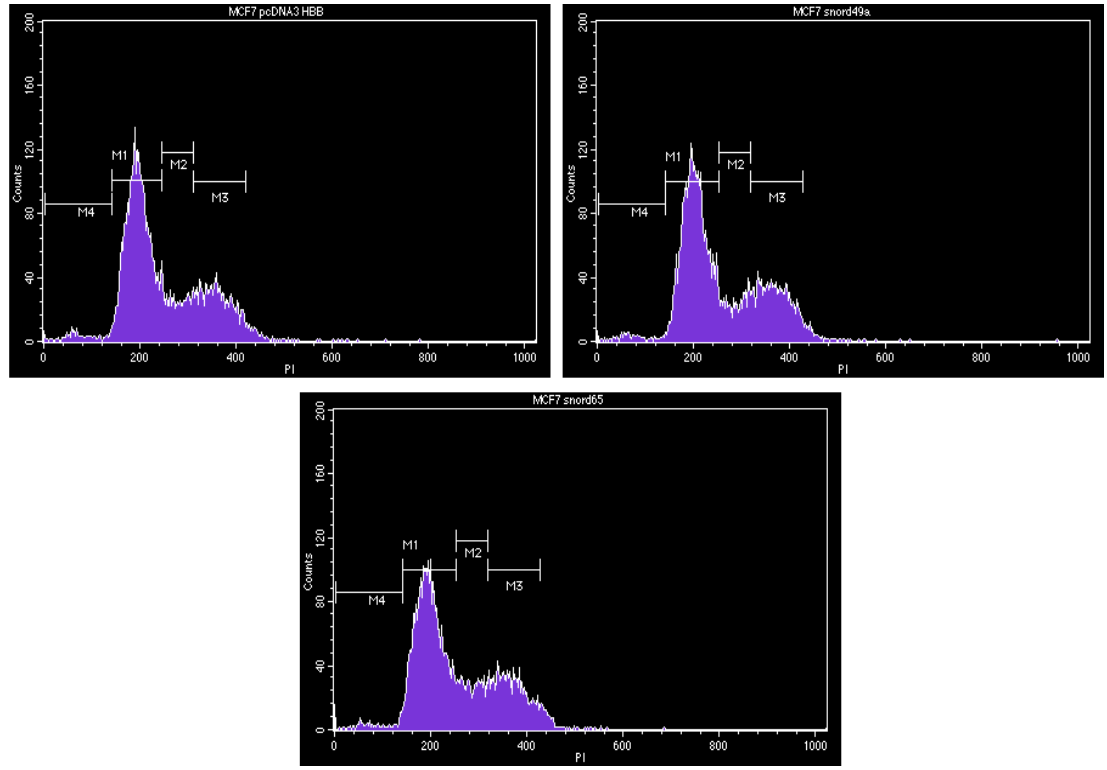

Figure 5.20. Cell cycle analysis for different cell lines (cont.). (g) MCF-7 24h. Stages indicated with M4,M1,M2 and M3 corresponded to sub-G1, G1, S and G2, respectively.

Cell cycle analysis for MCF-7 at 24 hours also indicated no difference for all samples (Figure 5.21, g). In addition to this, 48 hours analysis for MCF-7 was also performed with two independent experiments as other cell lines; however both attempts for analysis could not be reached to the final. Because peaks indicating G2 stage could not be obtained for any samples properly, the results were untrustable and this analysis was excluded from the study.

All of the results showed that snoRNA of *c17orf45* gene had no apperant effetcs on cell cycle stages of 4 different cancerous cell lines at 24 and 48 hours. Besides, the graphical representations of the analysis and percentages of each cell cycle stage for all cell lines could be attained in Figure 5.22 and in Table 5.4, respectively.

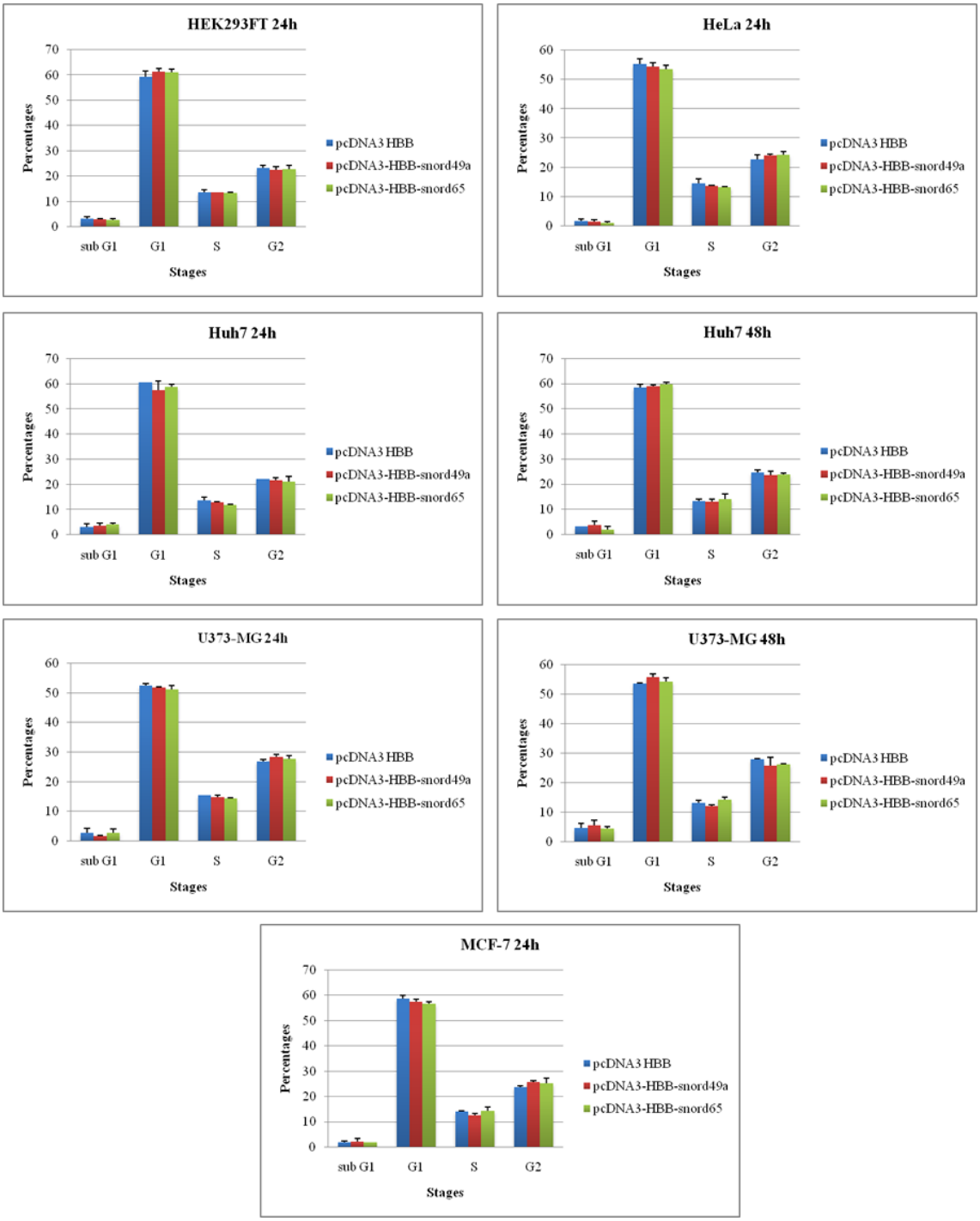

Figure 5.22. Graphical representation of cell cycle analysis results. The graphs indicate the results of two independent experiments.

Table 5.4. Percentages of the cells in cell cycle stages. The results indicated the average values of two independent experiments.

HEK293FT 24h				
	sub G1	G1	S	G2
pcDNA3 HBB	3,2	59,3	13,6	23,1
pcDNA3-HBB-snord49a	2,9	61,2	13,6	22,4
pcDNA3-HBB-snord65	2,6	61,0	13,3	22,8

HeLa 24h				
	sub G1	G1	S	G2
pcDNA3 HBB	1,9	55,2	14,7	22,7
pcDNA3-HBB-snord49a	1,4	54,3	13,8	24,1
pcDNA3-HBB-snord65	1,2	53,6	13,3	24,3

Huh7 24h				
	sub G1	G1	S	G2
pcDNA3 HBB	3,0	60,5	13,6	22,1
pcDNA3-HBB-snord49a	3,6	57,4	12,8	21,7
pcDNA3-HBB-snord65	4,1	58,8	11,9	21,3

Huh7 48h				
	sub G1	G1	S	G2
pcDNA3 HBB	3,3	58,4	13,3	24,6
pcDNA3-HBB-snord49a	3,7	59,0	12,9	23,7
pcDNA3-HBB-snord65	2,0	59,7	14,2	23,8

U373-MG 24h				
	sub G1	G1	S	G2
pcDNA3 HBB	2,6	52,5	15,4	26,8
pcDNA3-HBB-snord49a	1,6	51,9	14,8	28,4
pcDNA3-HBB-snord65	2,7	51,2	14,3	27,8

U373-MG 48h				
	sub G1	G1	S	G2
pcDNA3 HBB	4,6	53,6	13,0	28,0
pcDNA3-HBB-snord49a	5,6	55,7	12,0	25,8
pcDNA3-HBB-snord65	4,5	54,1	14,1	26,2

MCF-7 24h				
	sub G1	G1	S	G2
pcDNA3 HBB	1,8	58,8	14,1	23,6
pcDNA3-HBB-snord49a	2,2	57,4	12,4	25,6
pcDNA3-HBB-snord65	1,8	56,6	14,2	25,3

6. DISCUSSION

Identification of the putative protein product of c*17orf45* gene and the effects of the snoRNAs residing in the introns of this gene in terms of cell cycle progression in different cancer cell lines were analyzed in this study. Previously, SAGE and microarray analyses performed in our laboratory were done to identify and characterize the novel transcriptional targets of Wnt/β-catenin signaling pathway. Among approximately 100 candidate genes, some of them including *c17orf45* gene were identified and indicated as Wnt target (Şeker, 2009). In similar context, a bioinformatics program called oncoreveal which was designed by our former lab member to pick or compare candidate genes having a differential expression in different tumor samples indicated that the expression level of *c17orf45* gene changed in different tumor types (Kavak, 2009). In addition to these, it had been indicated that the construct containing ORF of *c17orf45* gene inhibited the proliferation of U373-MG (Şeker, 2009) and colony formation of 18kj40 cells (Kavak, 2009). Furthermore, there are 3 snoRNAs located in introns of *c17orf45* gene and recently, the relationship between snoRNAs and cancer become clearer (Mannoor *et al.,* 2012, Williams and Farzaneh, 2012). In this context, analyzing of putative protein product of the gene and the impacts of snoRNAs seem very vital to go a step further in cancer research.

Firstly, bioinformatics analyses were performed for putative ORF of the gene in this work. The conservation of open reading frame among distinct species was examined. Putative ORF of the gene was extracted from Genome Browser (uc002gqc.3). The homology for the gene was determined by obtaining sequences of other spaces via Blat search. Blat search pointed out that the sequence was only observed within primates. Similar analysis was performed for snoRNAs (snord49a and snord65) of the gene. SnoRNAs seemed much more conserved compared to ORF (Figure 5.3) (also mentioned in Şeker, 2009). In addition to this, phylogenetic trees were constructed for putative ORF. Two trees were designed; one of them was containing the sequences without considering the stop codon which led to shorter protein. Second tree was constructed with the sequences having stop codon and therefore included possibly functional pro-

teins. According to these two phylogenetic trees, second tree indicated a tree similar to primate evolution (Figure 5.2). by moving gorilla branch close to the ancestral point. Besides, gibbon was removed from analysis because the functional ORF of this species gave very short sequence (~60 bp). Because analysis was performed with complete deletion which deletes nonaligned sequences from all species, it was better to exclude this sequence. If gibbon sequence was used, it would result in very short sequences for all species and this would possibly affect the tree. Ultimately, phylogenetic tree analysis indicated that ORF of the gene was only conserved in primates and sno-RNAs of the gene were more conserved within the vertebrates.

Second, PAML analysis was performed. PAML was performed to indicate the ratio of the nonsynonymous over synonymous substitution (dN/dS=ω) on codons of ORF. By this ratio, the selective pressure on the gene could be determined. According to the results of one ratio model which implied the overall dN/dS ratio, there might be a possible positive selection on ORF of the gene indicating functional mutations. Free ratio model analysis was also performed and the dN/dS ratio was determined for each unique branch (Figure 5.5). Nevertheless, the free ratio model does not significantly fit for dN/dS data. Still, the ratio of the branch after gibbon towards human (ω=37.2352) seemed there might be positive selection on the gene; however the short length of the analyzed sequences could mask statistical reliability of the test. Besides, the sequences used for the species including baboon, rhesus, marmoset and squirrel monkey contained non funcional (non coding) part of the gene because stop codons were removed for running the program. Inclusion of non coding part gained neutral selection to the gene on these species which meant the deletion of these part had no biological importance. Then, one ratio model was applied with fixed ω values. ω values below 1 pointed out negative (natural) selection. Applying these dN/dS ratio to whole tree not only indicate these non coding parts as if it was under negative (natural) selection but also forced the positive selection on the gene if this really existed. The results of the test with the omega values varying between 0.1 and 0.5 showed significant results for positive selection of the gene (Table 5.2). All of these were the indicator of putative protein product of *c17orf45* gene.

As a first step to identify the protein product, commercially available antibody was obtained. After obtaining antibody, the basal level of c17orf45 protein was determined via Western Blot. Different cell lines were used to check protein product. As in Figure 5.6, the bands for the putative protein were obtained around 35 kDa and 70 kDa. According to GenBank (NM_152350.3, the suppressed sequence) and Genome Browser (uc002gqc.3) databases, the gene encodes 130 aa protein. This corresponds to around 15 kDa protein weight. Therefore, 35 kDa protein band acquired from different cell lines could be the possible protein product. This difference might results from a potential post-translational modification on protein. 70 kDa band was considered as unspecific band.

Next step for the analysis of protein was to overexpress the gene. To do this, two different overexpression constructs for the gene were utilized. Protein levels were determined after 48 hours post transfection for accumulation of protein. The bands were obtained around 35 kDa; however the thicker band which should represent the overexpression could not be obtained (Figure 5.7). Besides, beta-actin levels which indicated as loading control were also determined. Those were nearly equal as it was expected.

In addition to direct overexpression analysis, proteins were overexpressed with tagged constructs. GFP fused c17orf45 protein and myc-tagged c17orf45 proteins were analyzed. The proteins were visualized with anti-c17orf45, anti-GFP and anti-myc antibodies. Samples observed with anti-c17orf45 gene gave 35 kDa protein band which was consistent with previous finding; nevertheless samples visualized with anti-myc antibody gave 26 kDa band which was inconsistent as shown in Figure 5.8. Likewise, the sample including only GFP overexpression showed 35 kDa band which was possible the basal c17orf45 protein when visualized with anti-c17orf45 antibody. Same sample indicated 27 kDa protein band which was GFP overexpression when visualized with anti-GFP antibody. c17orf45-GFP overexpressed sample pointed to different protein bands. The uppermost band was around 48 kDa and this was lighter than possible c17orf45-GFP fused protein. However, this might also proceed from probable conformational change of fused protein and because of that the fused protein could moved faster. On the other hand, same sample did not indicate any protein band with anti-GFP

antibody which might result from the conformational change of fused protein by masking the epitope region required for antibody recognition (Figure 5.9). So, the comparison between these two cannot be concluded. All of these contradictory results indicated that anti-c17orf45 antibody possible did not target putative c17orf45 protein.

Although it was supposed that anti-c17orf45 protein did not target putative c17orf45 protein, immunoprecipitation was performed to obtain 35 kDa protein band to be sent to mass spectrometry. Western Blot following immunoprecipitation indicated the proper protein band around 35 kDa (Figure 5.10). Same sample was also stained with Coomassie Blue (Figure 5.11). The band was sent for mass spectrometry analysis. The results of mass spectrometry highly likely stated that anti-c17orf45 did not recognize putative protein (Table 5.3). In addition to this, mass spectrometry results pointed out mainly ribosomal proteins. This was consistent with the results of Western Blot analysis that protein obtained with anti-c17orf45 antibody was seen for all used cell lines. Different cell lines revealed same amount of protein as basal level. It might result from because of recognition of ribosomal proteins by this antibody. On the other hand, it could not be concluded whether *c17orf45* gene is protein coding or not. To finalize it, peptide design for new antibody production targeting putative c17orf45 protein is currently in progress.

In addition to c17orf45 protein works, intron encoded snoRNAs of the gene were studied. Apart from protein product of the gene, the possible effects of snoRNAs on different cancer cells were analyzed. In many studies, it has been show that processing of intronic snoRNAs depends on splicing (Kiss and Filipowicz, 1993, Kiss and Filipowicz, 1995). Previously in our lab, snoRNAs of *c17orf45* gene were cloned into intron of its own host gene, however overexpression of spliced version of *c17orf45* mRNA was not observed. Hence, snoRNAs were cloned into intronic region of *beta-globin* residing between two consecutive exons. Splicing out and proper processing of snoRNAs from nonhost intron when cloned within *beta-globin* gene has been previously realized (Darzacq and Kiss, 2000, Kiss and Filipowicz, 1995). Therefore, two snoRNAs of *c17orf45* gene, snord49a and snord65, were cloned into intronic region of *HBB* gene. Small parts of exons were cloned to provide the activation of splicing ma-

chinery and these regions were theoretically enough for splicing. Following RNA isolation and cDNA synthesis, RT-PCR was applied to samples. According to RT-PCR results, spliced version of constructs indicated about 70 bp fragment (Figure 5.16). Interestingly, overexpression performed with pcDNA3 plasmid indicating basal level of spliced *HBB* mRNA was observed slightly below level than overexpressed samples. It might be explained with the exclusion of a prat of exonic region from basal level of mRNA; nevertheless HBB gene has consensus sequences required for splicing (Krainer et al., 1984). Likewise, overexpression of snord49a and snord65 was also observed (Figure 5.18). These increases in snoRNA levels implied either snoRNAs in pre-mRNA or processed snoRNAs. Latter was more plausible because splicing was properly observed. In addition to RT-PCR, Real Time PCR was performed. Results of Real Time PCR supported overexpression of spliced *HBB* mRNA and snoRNAs quantitatively. Spliced mRNAs were upregulated about 6 fold and this increase were around 13 and 18 fold for snoRNA samples compared to control group. Besides, removal of intronic region (~1000 bp) residing between exons had to occur under 5 sec. of elongation time for proper running of Real Time PCR. This was also another verification of splicing. Other than RT and Real Time PCR, splicing of mRNA was examined with YFP fused spliced peptide of *HBB*. Removal of introns and joining exons would cause YFP expression. Otherwise, intronic stop codons would lead to termination of translation. YFP expression was smoothly seen for both constructs (Figure 5.20). YFP expression observed under fluorescent microscopy was also another sign of splicing.

Validation of spliced constructs provided to analyze whether snoRNAs had any effects on different cancer cells. To examine this, cell cycle analyses were performed. Various cancer cell lines, which were HeLa, Huh7, MCF-7 and U373-MG and a non-cancerous, epithelial cell line, HEK293FT, were used. Two time points were applied, 24 and 48 hours. Because the duplication time of HeLa and HEK293FT were relatively short (~24 hours), analysis of cell cycle for these two cell lines were performed 24 hours post transfection. Otherwise, fully confluent cells on the plate would possibly affect the stages of cell cycle. Confluent cells might undergo stress and it would trigger many other cellular responses instead of direct effects of snoRNAs. For other two lines, which were Huh7 and U373-MG, analyses were performed for 24 and 48 hours after transfec-

tion. Besides, pcDNA-HBB construct which included only exonic and intronic regions of *HBB* gene were used the control of pcDNA3-HBB-snoRNA construct. By doing this, it could be speculated that any difference between control and experimental group in the analysis would result directly from the existence of snoRNAs. Hence, when the results of the cell cycle analysis were examined, it could be seen that there was no alteration on the stages among control and experimental groups for all cell lines. It may result from that although the splicing of HBB-snoRNA constructs was observed, the processing for snoRNAs might not occur. In other words, functional snoRNAs might not be obtained by the construct. Hence, splicing of *HBB* mRNA which led to small portion of peptide might not affect the cell cycle stages. Processed version of snoRNA which resulted in the regular secondary structure and functional snoRNA should be analyzed primarily. Furthermore, snoRNAs might be degraded within very short time in the cell and the effects of snoRNAs could not be seen. Besides, the analysis time might be very early to observe cellular responses arise from snoRNA presence. Especially, 24 hours after transfection might be very limited time to observe any significant change like proliferation and apoptosis in the cell. 48 hour could be accepted as more plausible time point for analysis. On the other hand, longer time points than 48 hours might help to reveal the possible impacts of snoRNAs but this might also led to a confusion whether the probable effect resulted from the existence of snoRNA or cells reaching to full confluency.

SnoRNAs have been showed that they have mostly tissue specific expression (Chang *et al.,* 2002). The expression of snoRNA might give an idea about the possible function of snoRNA. In a mouse study, it had been showed that some of mouse snoRNAs were expressed high in brain and had differential expression during fear and learning (Rogelj *et al.,* 2003). In a similar way, the expression analysis of snoRNA in different tissue and cancer form of that tissue might provide the possible effect of snoRNA on that type of cancer. Hence, determining the expression levels of snoRNAs of *c17orf45* in different tissue and cancer cells could help to specify the possible effects of snoRNAs.

Similar to tissue specific snoRNA expression of *c17orf45* gene, differential expression of ORF of *c17orf45* gene was observed in brain tumors (Kavak, 2009, Şeker, 2009). In addition, being the novel target of Wnt / β-catenin signaling, the conservation of ORF within only primates, the results of PAML analysis and the direct effects of ORF on brain cancer cells (inhibition of proliferation on U373-MG and inhibition of colony formation in 18kj40 cells) increased the probability of being a protein-coding gene of *c17orf45* which had a possible function on brain and/or brain tumor development.

REFERENCES

Aberle, H., A. Bauer, J. Stappert, A. Kispert and R. Kemler, 1997, "Beta-Catenin Is a Target for the Ubiquitin-Proteasome Pathway", *The EMBO Journal*, Vol. 16, No. 13, pp. 3797-3804.

Artimo, P., M. Jonnalagedda, K. Arnold, D. Baratin, G. Csardi, E. de Castro, S. Duvaud, V. Flegel, A. Fortier, E. Gasteiger, A. Grosdidier, C. Hernandez, V. Ioannidis, D. Kuznetsov, R. Liechti, S. Moretti, K. Mostaguir, N. Redaschi, G. Rossier, I. Xenarios and H. Stockinger, 2012, "Expasy: Sib Bioinformatics Resource Portal", *Nucleic Acids Research*, Vol. 40, No. W1, pp. W597-W603.

Askarian-Amiri, M.E., J. Crawford, J.D. French, C.E. Smart, M.A. Smith, M.B. Clark, K. Ru, T.R. Mercer, E.R. Thompson, S.R. Lakhani, A.C. Vargas, I.G. Campbell, M.A. Brown, M.E. Dinger and J.S. Mattick, 2011, "Snord-Host Rna Zfas1 Is a Regulator of Mammary Development and a Potential Marker for Breast Cancer", *RNA*, Vol. 17, No. 5, pp. 878-891.

Bachellerie, J.P., J. Cavaille and A. Huttenhofer, 2002, "The Expanding Snorna World", *Biochimie*, Vol. 84, No. 8, pp. 775-790.

Bortolin, M.L., P. Ganot and T. Kiss, 1999, "Elements Essential for Accumulation and Function of Small Nucleolar Rnas Directing Site-Specific Pseudouridylation of Ribosomal Rnas", *The EMBO Journal*, Vol. 18, No. 2, pp. 457-469.

Both, J., T. Wu, J. Bras, G.R. Schaap, F. Baas and T.J. Hulsebos, 2012, "Identification of Novel Candidate Oncogenes in Chromosome Region 17p11.2-P12 in Human Osteosarcoma", *PloS One*, Vol. 7, No. 1, p. e30907.

Brameier, M., A. Herwig, R. Reinhardt, L. Walter and J. Gruber, 2011, "Human Box C/D Snornas with Mirna Like Functions: Expanding the Range of Regulatory Rnas", *Nucleic Acids Research*, Vol. 39, No. 2, pp. 675-686.

Bratkovic, T. and B. Rogelj, 2011, "Biology and Applications of Small Nucleolar Rnas", *Cellular and Molecular Life Sciences : CMLS*, Vol. 68, No. 23, pp. 3843-3851.

Brocardo, M. and B.R. Henderson, 2008, "Apc Shuttling to the Membrane, Nucleus and Beyond", *Trends in Cell Biology*, Vol. 18, No. 12, pp. 587-596.

Cavaille, J. and J.P. Bachellerie, 1996, "Processing of Fibrillarin-Associated Snornas from Pre-Mrna Introns: An Exonucleolytic Process Exclusively Directed by the Common Stem-Box Terminal Structure", *Biochimie*, Vol. 78, No. 6, pp. 443-456.

Chang, L.S., S.Y. Lin, A.S. Lieu and T.L. Wu, 2002, "Differential Expression of Human 5s Snorna Genes", *Biochemical and Biophysical Research Communications*, Vol. 299, No. 2, pp. 196-200.

Chen, W., D. ten Berge, J. Brown, S. Ahn, L.A. Hu, W.E. Miller, M.G. Caron, L.S. Barak, R. Nusse and R.J. Lefkowitz, 2003, "Dishevelled 2 Recruits Beta-Arrestin 2 to Mediate Wnt5a-Stimulated Endocytosis of Frizzled 4", *Science*, Vol. 301, No. 5638, pp. 1391-1394.

Clevers, H., 2006, "Wnt/Beta-Catenin Signaling in Development and Disease", *Cell*, Vol. 127, No. 3, pp. 469-480.

Darzacq, X. and T. Kiss, 2000, "Processing of Intron-Encoded Box C/D Small Nucleolar Rnas Lacking a 5',3'-Terminal Stem Structure", *Molecular and Cellular Biology*, Vol. 20, No. 13, pp. 4522-4531.

Dong, X.Y., P. Guo, J. Boyd, X. Sun, Q. Li, W. Zhou and J.T. Dong, 2009, "Implication of Snorna U50 in Human Breast Cancer", *Journal of Genetics and Genomics = Yi Chuan Xue Bao*, Vol. 36, No. 8, pp. 447-454.

Dong, X.Y., C. Rodriguez, P. Guo, X. Sun, J.T. Talbot, W. Zhou, J. Petros, Q. Li, R.L. Vessella, A.S. Kibel, V.L. Stevens, E.E. Calle and J.T. Dong, 2008, "Snorna U50 Is a Candidate Tumor-Suppressor Gene at 6q14.3 with a Mutation Associated with

Clinically Significant Prostate Cancer", *Human Molecular Genetics*, Vol. 17, No. 7, pp. 1031-1042.

Ender, C., A. Krek, M.R. Friedlander, M. Beitzinger, L. Weinmann, W. Chen, S. Pfeffer, N. Rajewsky and G. Meister, 2008, "A Human Snorna with Microrna-Like Functions", *Molecular Cell*, Vol. 32, No. 4, pp. 519-528.

Felsenstein, J., 1985, "Confidence-Limits on Phylogenies - an Approach Using the Bootstrap", *Evolution*, Vol. 39, No. 4, pp. 783-791.

Ganot, P., M.L. Bortolin and T. Kiss, 1997, "Site-Specific Pseudouridine Formation in Preribosomal Rna Is Guided by Small Nucleolar Rnas", *Cell*, Vol. 89, No. 5, pp. 799-809.

Gerhard, D.S., L. Wagner, E.A. Feingold, C.M. Shenmen, L.H. Grouse, G. Schuler, S.L. Klein, S. Old, R. Rasooly, P. Good, M. Guyer, A.M. Peck, J.G. Derge, D. Lipman, F.S. Collins, W. Jang, S. Sherry, M. Feolo, L. Misquitta, E. Lee, K. Rotmistrovsky, S.F. Greenhut, C.F. Schaefer, K. Buetow, T.I. Bonner, D. Haussler, J. Kent, M. Kiekhaus, T. Furey, M. Brent, C. Prange, K. Schreiber, N. Shapiro, N.K. Bhat, R.F. Hopkins, F. Hsie, T. Driscoll, M.B. Soares, T.L. Casavant, T.E. Scheetz, M.J. Brown-stein, T.B. Usdin, S. Toshiyuki, P. Carninci, Y. Piao, D.B. Dudekula, M.S. Ko, K. Kawakami, Y. Suzuki, S. Sugano, C.E. Gruber, M.R. Smith, B. Simmons, T. Moore, R. Waterman, S.L. Johnson, Y. Ruan, C.L. Wei, S. Mathavan, P.H. Gunaratne, J. Wu, A.M. Garcia, S.W. Hulyk, E. Fuh, Y. Yuan, A. Sneed, C. Kowis, A. Hodgson, D.M. Muzny, J. McPherson, R.A. Gibbs, J. Fahey, E. Helton, M. Ketteman, A. Madan, S. Rodrigues, A. Sanchez, M. Whiting, A. Madari, A.C. Young, K.D. Wetherby, S.J. Granite, P.N. Kwong, C.P. Brinkley, R.L. Pearson, G.G. Bouffard, R.W. Blakesly, E.D. Green, M.C. Dickson, A.C. Rodriguez, J. Grimwood, J. Schmutz, R.M. Myers, Y.S. Butterfield, M. Griffith, O.L. Griffith, M.I. Krzywinski, N. Liao, R. Morin, D. Palmquist, A.S. Petrescu, U. Skalska, D.E. Smailus, J.M. Stott, A. Schnerch, J.E. Schein, S.J. Jones, R.A. Holt, A. Baross, M.A. Marra, S. Clifton, K.A. Makowski, S. Bosak and J. Malek, 2004, "The Status, Quality, and Expansion of the Nih Full-Length Cdna Project: The Mammalian Gene Collection (Mgc)", *Genome Research*, Vol. 14, No. 10B, pp. 2121-2127.

He, T.C., A.B. Sparks, C. Rago, H. Hermeking, L. Zawel, L.T. da Costa, P.J. Morin, B. Vogelstein and K.W. Kinzler, 1998, "Identification of C-Myc as a Target of the Apc Pathway", *Science*, Vol. 281, No. 5382, pp. 1509-1512.

Huang, G.M., A. Jarmolowski, J.C. Struck and M.J. Fournier, 1992, "Accumulation of U14 Small Nuclear Rna in Saccharomyces Cerevisiae Requires Box C, Box D, and a 5', 3' Terminal Stem", *Molecular and Cellular Biology*, Vol. 12, No. 10, pp. 4456-4463.

Huttenhofer, A., M. Kiefmann, S. Meier-Ewert, J. O'Brien, H. Lehrach, J.P. Bachellerie and J. Brosius, 2001, "RNomics: an Experimental Approach That Identifies 201 Candidates for Novel, Small, Non-messenger RNAs in Mouse", *The EMBO Journal*, Vol. 20, No. 11, pp. 2943-2953.

Kavak, E., 2009, *Defining Novel Cancer Genes, Sage Tags and Co-Regulated Regions of the Human Genome Evolving from the Search and Identification of Novel Wnt/Tcf/Beta-Catenin Targets*, Ph.D. Thesis, Bogazici University.

Kavak, E., M. Unlu, M. Nister and A. Koman, 2010, "Meta-Analysis of Cancer Gene Expression Signatures Reveals New Cancer Genes, Sage Tags and Tumor Associated Regions of Co-Regulation", *Nucleic Acids Research*, Vol. 38, No. 20, pp. 7008-7021.

Kent, W.J., 2002, "Blat--the Blast-Like Alignment Tool", *Genome Research*, Vol. 12, No. 4, pp. 656-664.

Kimura, M., 1980, "A Simple Method for Estimating Evolutionary Rates of Base Substitutions through Comparative Studies of Nucleotide Sequences", *Journal of Molecular Evolution*, Vol. 16, No. 2, pp. 111-120.

Kino, T., D.E. Hurt, T. Ichijo, N. Nader and G.P. Chrousos, 2010, "Noncoding Rna Gas5 Is a Growth Arrest- and Starvation-Associated Repressor of the Glucocorticoid Receptor", *Science Signaling*, Vol. 3, No. 107, p. ra8.

Kishore, S. and S. Stamm, 2006, "The Snorna Hbii-52 Regulates Alternative Splicing of the Serotonin Receptor 2c", *Science*, Vol. 311, No. 5758, pp. 230-232.

Kiss-Laszlo, Z., Y. Henry, J.P. Bachellerie, M. Caizergues-Ferrer and T. Kiss, 1996, "Site-Specific Ribose Methylation of Preribosomal Rna: A Novel Function for Small Nucleolar Rnas", *Cell*, Vol. 85, No. 7, pp. 1077-1088.

Kiss, T. and W. Filipowicz, 1993, "Small Nucleolar Rnas Encoded by Introns of the Human Cell Cycle Regulatory Gene Rcc1", *The EMBO Journal*, Vol. 12, No. 7, pp. 2913-2920.

Kiss, T. and W. Filipowicz, 1995, "Exonucleolytic Processing of Small Nucleolar Rnas from Pre-Mrna Introns", *Genes & Development*, Vol. 9, No. 11, pp. 1411-1424.

Klaus, A. and W. Birchmeier, 2008, "Wnt Signalling and Its Impact on Development and Cancer", *Nature Reviews. Cancer*, Vol. 8, No. 5, pp. 387-398.

Krainer, A.R., T. Maniatis, B. Ruskin and M.R. Green, 1984, "Normal and Mutant Human Beta-Globin Pre-Mrnas Are Faithfully and Efficiently Spliced in Vitro", *Cell*, Vol. 36, No. 4, pp. 993-1005.

Larkin, M.A., G. Blackshields, N.P. Brown, R. Chenna, P.A. McGettigan, H. McWilliam, F. Valentin, I.M. Wallace, A. Wilm, R. Lopez, J.D. Thompson, T.J. Gibson and D.G. Higgins, 2007, "Clustal W and Clustal X Version 2.0", *Bioinformatics*, Vol. 23, No. 21, pp. 2947-2948.

Lestrade, L. and M.J. Weber, 2006, "SnoRNA-LBME-db, a Comprehensive Database of Human H/ACA and C/D Box SnoRNAs", *Nucleic Acids Research*, Vol. 34, Database issue, pp. D158-162.

Li, R., H. Wang, B.N. Bekele, Z. Yin, N.P. Caraway, R.L. Katz, S.A. Stass and F. Jiang, 2006, "Identification of Putative Oncogenes in Lung Adenocarcinoma by a Comprehensive Functional Genomic Approach", *Oncogene*, Vol. 25, No. 18, pp. 2628-2635.

Liu, W., X. Dong, M. Mai, R.S. Seelan, K. Taniguchi, K.K. Krishnadath, K.C. Halling, J.M. Cunningham, L.A. Boardman, C. Qian, E. Christensen, S.S. Schmidt, P.C. Roche, D.I.

Smith and S.N. Thibodeau, 2000, "Mutations in Axin2 Cause Colorectal Cancer with Defective Mismatch Repair by Activating Beta-Catenin/Tcf Signalling", *Nature Genetics*, Vol. 26, No. 2, pp. 146-147.

Mannoor, K., J. Liao and F. Jiang, 2012, "Small Nucleolar Rnas in Cancer", *Biochimica et Biophysica Acta*, Vol. 1826, No. 1, pp. 121-128.

Mao, J., J. Wang, B. Liu, W. Pan, G.H. Farr, 3rd, C. Flynn, H. Yuan, S. Takada, D. Kimelman, L. Li and D. Wu, 2001, "Low-Density Lipoprotein Receptor-Related Protein-5 Binds to Axin and Regulates the Canonical Wnt Signaling Pathway", *Molecular Cell*, Vol. 7, No. 4, pp. 801-809.

Mei, Y.P., J.P. Liao, J. Shen, L. Yu, B.L. Liu, L. Liu, R.Y. Li, L. Ji, S.G. Dorsey, Z.R. Jiang, R.L. Katz, J.Y. Wang and F. Jiang, 2012, "Small Nucleolar Rna 42 Acts as an Oncogene in Lung Tumorigenesis", *Oncogene*, Vol. 31, No. 22, pp. 2794-2804.

Meyer, L.R., A.S. Zweig, A.S. Hinrichs, D. Karolchik, R.M. Kuhn, M. Wong, C.A. Sloan, K.R. Rosenbloom, G. Roe, B. Rhead, B.J. Raney, A. Pohl, V.S. Malladi, C.H. Li, B.T. Lee, K. Learned, V. Kirkup, F. Hsu, S. Heitner, R.A. Harte, M. Haeussler, L. Guruvadoo, M. Goldman, B.M. Giardine, P.A. Fujita, T.R. Dreszer, M. Diekhans, M.S. Cline, H. Clawson, G.P. Barber, D. Haussler and W.J. Kent, 2013, "The Ucsc Genome Browser Database: Extensions and Updates 2013", *Nucleic Acids Research*, Vol. 41, No. Database issue, pp. D64-69.

Molenaar, M., M. van de Wetering, M. Oosterwegel, J. Peterson-Maduro, S. Godsave, V. Korinek, J. Roose, O. Destree and H. Clevers, 1996, "Xtcf-3 Transcription Factor Mediates Beta-Catenin-Induced Axis Formation in Xenopus Embryos", *Cell*, Vol. 86, No. 3, pp. 391-399.

Nei, M. and T. Gojobori, 1986, "Simple Methods for Estimating the Numbers of Synonymous and Nonsynonymous Nucleotide Substitutions", *Molecular Biology and Evolution*, Vol. 3, No. 5, pp. 418-426.

Nishisho, I., Y. Nakamura, Y. Miyoshi, Y. Miki, H. Ando, A. Horii, K. Koyama, J. Utsunomiya, S. Baba and P. Hedge, 1991, "Mutations of Chromosome 5q21 Genes in Fap and Colorectal Cancer Patients", *Science*, Vol. 253, No. 5020, pp. 665-669.

Nusse, R., 2008, "Wnt Signaling and Stem Cell Control", *Cell Research*, Vol. 18, No. 5, pp. 523-527.

Ono, M., M.S. Scott, K. Yamada, F. Avolio, G.J. Barton and A.I. Lamond, 2011, "Identification of Human Mirna Precursors That Resemble Box C/D Snornas", *Nucleic Acids Research*, Vol. 39, No. 9, pp. 3879-3891.

Page, R.D.M., 1996, "Treeview: An Application to Display Phylogenetic Trees on Personal Computers", *Computer Applications in the Biosciences*, Vol. 12, No. 4, pp. 357-358.

Polakis, P., 2000, "Wnt Signaling and Cancer", *Genes & Development*, Vol. 14, No. 15, pp. 1837-1851.

Rogelj, B., C.E. Hartmann, C.H. Yeo, S.P. Hunt and K.P. Giese, 2003, "Contextual Fear Conditioning Regulates the Expression of Brain-Specific Small Nucleolar Rnas in Hippocampus", *The European Journal of Neuroscience*, Vol. 18, No. 11, pp. 3089-3096.

Saitou, N. and M. Nei, 1987, "The Neighbor-Joining Method: A New Method for Reconstructing Phylogenetic Trees", *Molecular Biology and Evolution*, Vol. 4, No. 4, pp. 406-425.

Sakanaka, C., 2002, "Phosphorylation and Regulation of Beta-Catenin by Casein Kinase I Epsilon", *Journal of Biochemistry*, Vol. 132, No. 5, pp. 697-703.

Satoh, S., Y. Daigo, Y. Furukawa, T. Kato, N. Miwa, T. Nishiwaki, T. Kawasoe, H. Ishiguro, M. Fujita, T. Tokino, Y. Sasaki, S. Imaoka, M. Murata, T. Shimano, Y. Yamaoka and Y. Nakamura, 2000, "Axin1 Mutations in Hepatocellular Carcinomas, and Growth Suppression in Cancer Cells by Virus-Mediated Transfer of Axin1", *Nature Genetics*, Vol. 24, No. 3, pp. 245-250.

Scott, M.S., F. Avolio, M. Ono, A.I. Lamond and G.J. Barton, 2009, "Human Mirna Precursors with Box H/Aca Snorna Features", *PLoS Computational Biology*, Vol. 5, No. 9, p. e1000507.

Scott, M.S. and M. Ono, 2011, "From Snorna to Mirna: Dual Function Regulatory Non-Coding Rnas", *Biochimie*, Vol. 93, No. 11, pp. 1987-1992.

Scott, M.S., M. Ono, K. Yamada, A. Endo, G.J. Barton and A.I. Lamond, 2012, "Human Box C/D Snorna Processing Conservation across Multiple Cell Types", *Nucleic Acids Research*, Vol. 40, No. 8, pp. 3676-3688.

Smith, C.M. and J.A. Steitz, 1998, "Classification of Gas5 as a Multi-Small-Nucleolar-Rna (Snorna) Host Gene and a Member of the 5'-Terminal Oligopyrimidine Gene Family Reveals Common Features of Snorna Host Genes", *Molecular and Cellular Biology*, Vol. 18, No. 12, pp. 6897-6909.

Şeker, T., 2009, *Characterization of C17orf45 as a Novel Target of the Wnt/B-Catenin Pathway*, M.S. Thesis, Bogazici University.

Tamura, K., J. Dudley, M. Nei and S. Kumar, 2007, "Mega4: Molecular Evolutionary Genetics Analysis (Mega) Software Version 4.0", *Molecular Biology and Evolution*, Vol. 24, No. 8, pp. 1596-1599.

Tanaka, R., H. Satoh, M. Moriyama, K. Satoh, Y. Morishita, S. Yoshida, T. Watanabe, Y. Nakamura and S. Mori, 2000, "Intronic U50 Small-Nucleolar-Rna (Snorna) Host Gene of No Protein-Coding Potential Is Mapped at the Chromosome Breakpoint T(3;6)(Q27;Q15) of Human B-Cell Lymphoma", *Genes to Cells : Devoted to Molecular & Cellular Mechanisms*, Vol. 5, No. 4, pp. 277-287.

Valdivia, L.E., R.M. Young, T.A. Hawkins, H.L. Stickney, F. Cavodeassi, Q. Schwarz, L.M. Pullin, R. Villegas, E. Moro, F. Argenton, M.L. Allende and S.W. Wilson, 2011, "Lef1-Dependent Wnt/Beta-Catenin Signalling Drives the Proliferative Engine That Maintains Tissue Homeostasis During Lateral Line Development", *Development*, Vol. 138, No. 18, pp. 3931-3941.

Vitali, P., E. Basyuk, E. Le Meur, E. Bertrand, F. Muscatelli, J. Cavaille and A. Huttenhofer, 2005, "Adar2-Mediated Editing of Rna Substrates in the Nucleolus Is Inhibited by C/D Small Nucleolar Rnas", *The Journal of Cell Biology*, Vol. 169, No. 5, pp. 745-753.

Williams, G.T. and F. Farzaneh, 2012, "Are Snornas and Snorna Host Genes New Players in Cancer?", *Nature Reviews. Cancer*, Vol. 12, No. 2, pp. 84-88.

Xie, J., M. Zhang, T. Zhou, X. Hua, L. Tang and W. Wu, 2007, "Sno/Scarnabase: A Curated Database for Small Nucleolar Rnas and Cajal Body-Specific Rnas", *Nucleic Acids Research*, Vol. 35, No. Database issue, pp. D183-187.

Yamashita, R., Y. Suzuki, N. Takeuchi, H. Wakaguri, T. Ueda, S. Sugano and K. Nakai, 2008, "Comprehensive Detection of Human Terminal Oligo-Pyrimidine (Top) Genes and Analysis of Their Characteristics", *Nucleic Acids Research*, Vol. 36, No. 11, pp. 3707-3715.

Yang, Z., 2007, "Paml 4: Phylogenetic Analysis by Maximum Likelihood", *Molecular Biology and Evolution*, Vol. 24, No. 8, pp. 1586-1591.

Yost, C., M. Torres, J.R. Miller, E. Huang, D. Kimelman and R.T. Moon, 1996, "The Axis-Inducing Activity, Stability, and Subcellular Distribution of Beta-Catenin Is Regulated in Xenopus Embryos by Glycogen Synthase Kinase 3", *Genes & Development*, Vol. 10, No. 12, pp. 1443-1454.

Zeng, X., H. Huang, K. Tamai, X. Zhang, Y. Harada, C. Yokota, K. Almeida, J. Wang, B. Doble, J. Woodgett, A. Wynshaw-Boris, J.C. Hsieh and X. He, 2008, "Initiation of Wnt Signaling: Control of Wnt Coreceptor Lrp6 Phosphorylation/Activation Via Frizzled, Dishevelled and Axin Functions", *Development*, Vol. 135, No. 2, pp. 367-375.